



Iron Speciation in Precipitation in the North-Eastern Mediterranean and Its Relationship with Sahara Dust

TÜRKAN ÖZSOY^{1*} and A. CEMAL SAYDAM²

¹*Mersin University, Science and Literature Faculty, Department of Chemistry, 33342, Mersin, İçel, Turkey*

²*Turkish Scientific and Technical Research Council (TÜBİTAK), Ankara, Turkey*

(Received: 15 August 2000; accepted: 15 January 2001)

Abstract. Precipitation samples collected at Erdemli, Turkey, during February 1996–June 1997 were analysed to determine iron content and speciation. The purpose of the measurements was to examine the atmospheric abundance of iron and to quantify its solubility in the region. Spectrophotometric analyses of Fe(II) and reducible Fe(III) in precipitation samples, along with measurements of pH, conductivity, filterable iron (Fe_{filt}), particulate aluminium (Al_{par}) and particulate iron (Fe_{par}) were performed to determine iron solubility, which principally affects its bioavailability. Backward trajectories corresponding to the sampling dates were analysed to determine the sources of atmospheric constituents arriving at the site. Among these, the mineral dust transported from the Great Sahara to the region is considered to be a rich source of iron. The concentration of Fe(II) varied from below detection limit ($0.02 \mu\text{M}$) up to $0.42 \mu\text{M}$, while the maximum concentration of total reactive Fe (referred as Fe(II) + reducible Fe(III) = Fe_{reac}) was found to be $1.0 \mu\text{M}$ in precipitation. A strong correlation was found between particulate Fe and Al fractions, both of crustal origin. No correlation was observed between the soluble and insoluble fractions of iron. The soluble iron fraction, Fe(II) concentration varied independently from the concentrations of reducible Fe(III), Fe_{filt} , Fe_{par} , and from the pH of the precipitation. The Fe_{filt} fraction (size $< 0.45 \mu\text{m}$), measured by Atomic Absorption Spectrophotometer, and frequently interpreted to be the soluble iron fraction in the literature, was found to be significantly higher than the corresponding Fe_{reac} fraction in precipitation samples, most likely due to the colloidal iron content of the Fe_{filt} fraction passing through the $0.45 \mu\text{m}$ pore size filter. The volume weighted mean Fe_{filt} concentration of the precipitation samples collected during the episodic ‘red rain’ events was found to be relatively higher. The geometric mean ratios of soluble Fe(II) and of Fe_{reac} to Total Fe ($Fe_{\text{filt}} + Fe_{\text{par}}$), were found to be 1.6% and 2.1%, respectively, while the mean ratio of Fe_{filt} to Total Fe was 9.6%. The flux of bioavailable iron (Fe_{reac}) fraction in most atmospheric wet deposition events was found to be sufficient for supporting the maximum primary production rates that are typical for the Eastern Mediterranean Sea.

Key words: Eastern Mediterranean, mineral dust, red rain, iron speciation, atmospheric soluble iron, wet deposition flux.

* Address for correspondence: Institute of Marine Sciences, Middle East Technical University, PO Box 28, Erdemli, 33731, İçel, Turkey, e-mail: turkan@ims.metu.edu.tr

1. Introduction

The abundance and solubility of iron in the atmosphere is important for the ocean because iron could be a limiting nutrient for marine primary productivity, especially in the HNLC (high nutrient low chlorophyll) regions (Martin and Fitzwater, 1988; Martin *et al.*, 1991) of the Antarctic and equatorial Pacific Oceans, where the deposition of dust, providing the source of iron, is at its lowest (Uematsu, 1987; Duce and Tindale, 1991). In contrast, the equatorial North Atlantic, which receives a large flux of Sahara dust (Prospero, 1981; Kremling and Streu, 1993), has sufficient iron resulting in complete assimilation of the available nutrients. Pulses of mineral aerosols originating from Africa reach the Mediterranean region, and their Fe content supposedly could contribute to marine biological production through time-dependent biogeochemical processes (Quetel *et al.*, 1993). In addition to its Fe content, the dust from Sahara contains ample quantities of other micro-nutrients, such as Zn, Mn and Co, Ni, Cu (Kubilay, 1996), and macro-nutrients, such as PO_4^{-3} (Talbot *et al.*, 1986; Bergametti *et al.*, 1992; Migon and Sandroni, 1999). The latter is known to be the limiting nutrient for phytoplankton production in the Mediterranean, and its atmospheric supply could have important consequences. While most studies have focused on the potential effects of individual metals, synergistic and antagonistic interactions between multiple trace metals could be very important on oceanic plankton production and species composition (Bruland *et al.*, 1991). These studies, confirming initiation of certain biogeochemical processes by oceanic dust deposition, has lead Donaghay *et al.* (1991) to suggest various scenarios of marine ecosystem responses to episodic atmospheric inputs of the nutrient elements. Sahara dust contains 5–30% of calcite (CaCO_3) (Loye-Pilot *et al.*, 1986), which in partial dissolution could increase the pH of rainwater, which in turn could supply dissolved inorganic carbon (DIC) to the ocean, to be used in the production of CaCO_3 (coccolith formation). Research conducted with pure iron minerals have strongly linked photochemical solubility of iron to its mineralogical structure (Sulzberger, 1992; Sulzberger and Laubscher, 1995). The verification of these existing hypotheses requires integrated research efforts on a much larger scale, involving simultaneous measurements of biogeochemical variables within the surface micro-layer of the ocean.

As a result of P limitation the Eastern Mediterranean marine environment is characterised with a high N:P ratio near the sea surface (Krom *et al.*, 1991). Iron limitation is generally not expected since a substantial amount of iron, especially in particulate form, is supplied from surrounding land, through atmospheric deposition or rivers in flow (Guieu *et al.*, 1991). On the other hand, iron bioavailability to phytoplankton could still be limited since they only utilise free (or reactive) soluble Fe species (Anderson and Morel, 1982), which, because of the extreme insolubility of Fe, typically constitute a small portion of the total Fe in oxic seawater. The bulk of Fe occurs in particulate and colloidal forms, which must dissolve to produce the soluble species assimilated by phytoplankton (Finden *et al.*, 1984; Rich and Morel,

1990; Wells *et al.*, 1991). Recent studies have revealed that the availability of iron to phytoplankton is controlled by ferric and ferrous ion activities, which in turn are controlled partially by complex redox cycle involving photo-reduction of ferric iron to soluble ferrous iron in either sea surface (Johnson *et al.*, 1994) or atmospheric waters (Erel *et al.*, 1993; Faust, 1994). The atmospheric photo-reduction, requires sunlight and moisture as well as iron particles; hence it is closely related with synoptic weather as well as cloud processes. Due to the very low solubility of iron minerals in natural waters (Zhu *et al.*, 1992) and thermodynamically unstable character of Fe(II) in the oxygenated waters, Fe(III) has been assumed to be the predominant species present in cloud water and aerosol particles (Pandis and Seinfeld, 1989). Though Fe(III) is the thermodynamically stable oxidation state of iron in oxic seawater, a substantial body of new evidence suggests that a significant fraction of dissolved iron in surface waters exists as Fe(II) (Wells *et al.*, 1995; Zhuang *et al.*, 1995; Sivan *et al.*, 1998). The deposition of photochemically altered aerosols may be a significant source of Fe(II) to surface waters. For example, high concentrations of Fe(II) has been measured in fog water (Behra and Sigg, 1990), in cloud aerosols (Zhu *et al.*, 1993) and in aerosols from remote ocean regions (Zhuang *et al.*, 1992; Zhu *et al.*, 1997). Such redox cycles within the clouds or rainwater containing dust particles would tend to influence both ferrous and ferric ion activities and therefore enhance iron availability which could trigger bloom formation when deposited on the ocean surface (Saydam, 1996; Guerzoni *et al.*, 1999).

In this study, we present Fe speciation measurements in precipitation samples, in conjunction with long-term monitoring (since 1991) of atmospheric aerosols at Erdemli on the Eastern Mediterranean coast of Turkey. In searching for the natural occurrence of iron in the area of investigation, this study aims to serve as an elementary step in the larger scale assessments of the biogeochemical impacts of desert dust. The results reached so far have demonstrated the temporal variability of aerosol dust, with a mean dust loading of $15.5 \pm 25 \mu\text{g m}^{-3}$ (Kubilay *et al.*, 2000), and the magnitude of wet deposition associated with cyclones, leading to an abrupt decrease of atmospheric dust load after washout by rain. Our purpose has been to determine the concentration level of soluble Fe(II) and Fe_{reac} in precipitation and its percentage within the total iron flux transported to the Eastern Mediterranean surface waters through wet deposition, and to identify differences, if any, of soluble iron wet deposition between 'normal' and 'red rain' precipitation events. The term 'red rain' refers to precipitation events coinciding with dust transport, identified by the reddish or yellowish color of membrane filters used in filtering the rainwater.

2. Materials and Methods

2.1. SAMPLING STATION

The sampling station is located on the harbor jetty of the Institute of Marine Sciences, METU (36°33'54" N and 34°15'18" E) on the south-eastern coast of Turkey (Figure 1). The two nearest urban centers are Erdemli (a small town with a population of 35.000) and Mersin (a big and industrialized city with more than 1.000.000 inhabitants) located 7 and 45 km east of the sampling site, respectively. Agricultural and tourist activity occurs in the close vicinity, while limited industrial activity such as petroleum refinery, thermal power and fertilizer plants, non-ferrous metal (chromium), pulp and paper and soda production occurs along the coast at distances of more than 50 km to the east and west of the sampling tower.

2.2. SAMPLING PROCEDURE

A total of 87 samples from precipitation events has been collected between 5 February 1996–13 June 1997 by a Wet/Dry Sampler Analyzer, Model ARS 1000, MTX Italy, S.p.A., installed on a tower at a height of 22 m above sea level. The system is comprised of two HDPE (high density polyethylene) buckets with 30 cm diameter; one for dry and the other for wet deposition samples. A rain sensor detects the first few rain drops and activates a motor, opening the lid of the wet sampler. Due to practical difficulties of access to the sampling tower; night samples have been collected with buckets of the same size deployed on the roof of the Institute and kept there for the duration of rain. Sampling buckets, bottles and all glassware used in the laboratory have been soaked in 1M HCL washing solution for 48 hours and rinsed with distilled, de-ionized water several times prior to usage. Precipitation samples collected for each event were brought to the laboratory immediately following the cessation of rain. They were filtered through a 0.45 μm pore size membrane filter (MFS, cellulose acetate, 47 mm diameter) by applying gentle negative pressure immediately after collection to avoid possible exchange between particulate and dissolved phases, and divided into aliquots to be used in different analyses. Subsamples of precipitation were transferred in rigorously cleansed polyethylene bottles.

2.3. SOLUBLE IRON MEASUREMENTS

Because of the expected rapid rate of Fe(II) oxidation after sampling, all measurements of soluble Fe(II) were performed within about 1/2 h of sample collection. Fe(II) was measured spectrophotometrically (Heaney and Davison, 1977) by adding 2,2'-bipyridine ($\text{C}_{10}\text{H}_8\text{N}_2$) to an aliquot from the filtered precipitation. Fe(II) forms a stable red colored complex ion with the reagent 2,2'-bipyridine for several hours in a pH range of 3–10. Acetic acid (CH_3COOH) – sodium acetate ($\text{CH}_3\text{COONa}\cdot 3\text{H}_2\text{O}$) buffer solution was used to adjust the final pH of the sample

solution. Acetate buffer held the pH of the final solution at 4.6. The Fe(II) measurements were performed by a Varian Techtron Model 635 UV-Visible Absorbance spectrophotometer at the wavelength of 519 nm, using a 10-cm cell. The molar extinction coefficients (ϵ) of the Fe(II) complexes were calculated to be 8400 ± 400 L mol⁻¹ cm⁻¹ in distilled water. This value is in close agreement with the values quoted in the literature of 8600 (Snell *et al.*, 1959) and 8400 (Box, 1984). No detectable interference was reported for the solutions even containing Fe(III) in high concentrations.

The concentration of Fe(II) was measured by the same procedure, after reduction of the Fe(III) with the addition of hydroxylamine hydrochloride (HONH₂Cl). The result of this measurement was the sum of soluble Fe(II) and reducible Fe(III) concentrations and this value is operationally defined in this paper as the total reactive Fe [referred as Fe_{reac} = Fe(II) + reducible Fe(III)] (Powell and Landing, 1994; Kester, 1994). Reducible Fe(III) was then calculated from the difference of Fe_{reac} and Fe(II) concentrations. From the standpoint of iron utilization by primary producers, the extremely labile soluble Fe(II) and the moderately available reducible Fe(III), within our classification of reactive iron are considered to be the most readily available soluble forms of iron within the iron pool reaching the marine environment (Anderson and Morel, 1982; Kester, 1994).

When sufficient sample was available, the stability of soluble Fe(II) ions in the laboratory has been determined as follows: The sample was kept in a glass bottle at room temperature and light, while Fe(II) and Fe_{reac} concentrations were measured every hour. Fe(II) and Fe_{reac} was found to be stable over 11 hours. On the 12th hour a rapid decrease was observed in Fe(II), while Fe_{reac} remained the same. It was often not possible to continue the experiment past this time, since we ran out of the precipitation sample. Despite the inadequacy of this experiment to serve as a full kinetic study characterizing Fe(II) oxidation, it ensured the stability of the applied analytical procedure with respect to soluble iron, in the period after sampling.

The same procedures have been applied to field blanks collected once every month (except July and August 1996, lacking any rain). Approximately 200 mL of distilled de-ionized water was poured into the cleaned sampling bucket and deployed at the same place where precipitation was sampled. After a short time, the field blank was collected in the same way as the rain sample, to yield a measure of the potential contamination from handling and exposure at the sampling site, as well as the contamination originating from the bucket, filtration system, de-ionized water and reagent solution. In addition to field blanks, laboratory blanks, including all reagents and de-ionized water, were analyzed routinely in correspondence to every collected precipitation sample. The concentration of field and laboratory blanks measured throughout the study were all below the detection limit (0.02 μ M for both Fe(II) and Fe_{reac}). In order to eliminate the effects of photochemical processes all experiments were conducted under illumination by fluorescent light.

The reproducibility of the spectrophotometric analytical procedure was established by performing seven replicate analyses of precipitation subsamples when

Table I. Comparison of the measured pH and Fe_{filt} (mg L^{-1}) values of WMO-PRL simulated acid precipitation samples with the certified values (in the parentheses)

Sample #	pH	Fe_{filt} (mg L^{-1})
1143	4.60 (4.49)	–
2369	3.40 (3.51)	–
3595	3.37 (3.53)	–
4704	–	0.080 (0.080)
5930	–	0.045 (0.041)

sufficient amount of sample was available. Analytical precision for $\text{Fe}(\text{II})$ and Fe_{reac} measurements in terms of coefficient of variation (CV) was found to be 2% and 3%, respectively.

2.4. pH AND CONDUCTIVITY MEASUREMENTS

The pH was measured by a Microprocessor pH-meter (WTW-Model pH537, accuracy of 0.01 pH units), calibrated by pH:6.94 and pH:3.97 standard buffer solutions before every measurement. The glass electrode was soaked in the sample container, while it was gently shaken, and the pH value was recorded only after the electrode became stable. The accuracy of the pH measurements has been tested by analyzing simulated acid rain samples prepared by the World Meteorological Organization (WMO) Precipitation Reference Laboratory (PRL) for inter-comparison. The measured pH values, together with the certified values are presented in Table I. The analytical accuracy of pH measurements was found to be better than 5% (Özsoy and Saydam, 2000).

Conductivity measurements have been performed with a Model 4070 Conductivity-Meter (Cole Palmer) which has a temperature range of $-30\text{ }^{\circ}\text{C}$ – $+150\text{ }^{\circ}\text{C}$ and a conductivity range of $0\text{--}20\text{ mS cm}^{-1}$. Due to technical problems, conductivity measurements could be performed only in 41 of the precipitation samples. The pH and conductivity have been measured immediately after filtration. Further laboratory pH measurements indicated that these parameters were stable over several days. Precipitation was recorded at a sampling rate of half an hour by an Anderrea Meteorological Station installed at the roof of the Institute.

2.5. FILTERABLE IRON (Fe_{filt}) MEASUREMENTS

There is considerable uncertainty regarding the solubility of dissolved iron in natural waters, due to its complicated chemistry in aqueous solution (Stumm and Lee, 1960). In the literature, the dissolved fraction of any trace element is generally

defined as any material that passed through a 0.4–0.5 μm filter and then acidified to pH near 2 (Johnson *et al.*, 1994). But this definition is somewhat uncertain, particularly for iron, because of the size range of the ubiquitous colloidal Fe(III) hydroxide particles (Lengweiler *et al.*, 1961) and the reduction of effective pore size by retained material (Sheldon, 1972) during filtration of all types of natural waters. Colloids are traditionally defined as particles in the 1 to 1000 nm size range. Therefore, the classical definition of dissolved iron will contain colloidal iron as well as dissolved iron (Mill, 1980; O'Sullivan *et al.*, 1991; Powell and Landing, 1994). As a result of analytical restrictions, it is almost impossible to distinguish what fraction of the dissolved Fe is colloidal and what fraction is truly dissolved. Erel (1991) reported that ultra-filtration or dialysis membrane are needed for a complete separation of dissolved elements from particulate fraction in acidic to neutral pH streams and lakes. Several studies have also argued that the actual dissolved iron in natural waters is the fraction that pass through 0.025 μm pore-size filters (De Haan *et al.*, 1985; De Haan and De Boer, 1986; Erel *et al.*, 1993; Sivan *et al.*, 1998). Regarding all these limitations, in this paper the iron fraction which pass through a 0.45 μm filter is referred to as 'filterable iron' (Fe_{filt}) to distinguish it from dissolved iron. According to the conventional and traditional definition, Fe_{filt} corresponds to the total dissolved iron fraction in precipitation (Zhuang *et al.*, 1990; Behra and Sigg, 1990; Duce and Tindale, 1991; Guieu *et al.*, 1993; Zhuang *et al.*, 1995)

Aliquots for Fe_{filt} analysis were preserved by acidification with 0.1 M HNO_3 and stored at 4 °C until analysis time. Fe_{filt} was analysed by a computer-controlled GBC-906 model (GBC Scientific Equipment Pty Ltd, Australia) Atomic Absorption Spectrometer (AAS) equipped with a GF 2000/3000 graphite Furnace Module, with the attachment of PAL3000 autosampler. The detection limit of Fe was 1 nM and the coefficient of variance of the analysis was, at most, 4%. Concentrations of Fe_{filt} in monthly field blanks were also determined and it was found that field blanks never exceeded 10% of the lowest Fe_{filt} value measured. The accuracy of the analytical results has been tested by analyzing simulated acid rain samples prepared by World Meteorological Organization (WMO) Precipitation Reference Laboratory (PRL) for intercomparison. Measured Fe_{filt} concentrations together with the certified values (in parenthesis) are presented in Table I and the accuracy was found to be better than 10% for Fe_{filt} .

2.6. PARTICULATE Fe (Fe_{par}) AND Al (Al_{par}) MEASUREMENTS

Before the preparation of samples for particulate Fe and Al analysis, the color of the insoluble fraction of precipitation samples collected on 0.45 μm pore size membrane filter was identified and classified according to the standard soil color chart, based on the Munsell System.

Membrane filter samples have been digested according to the procedure given in UNEP (1995), using a microwave digestion oven (Questron Corporation, Q45

EnviroPrep Model) for particulate Fe and Al analysis. Total (HF) decomposition method has been applied with little modification in the adjustment of the instrument's (microwave oven) power and timing. For this purpose, Hydrofluoric acid (HF, 48% Merck, ISO, analytical grade dissolution agent for silicates and other refractory oxides) and aqua regia (HNO_3 , 65% Merck suprapur:HCl 30% Merck suprapur, dissolution agent for mainly organic material) (1:3 v/v) mixture have been used. Boric acid (H_3BO_3 , Merck ISO, analytical grade) crystals have been added during dilution of digested samples with Millipore-Milli Q water in order to counter any corrosive effects by the tiniest amounts of HF. At least one Community Bureau of Reference Brussels (BCR) sample has been digested simultaneously with the membrane filter samples on every digestion set of samples in order to check the completeness of each digestion procedure. Digested samples were diluted to 50 mL volume by double distilled de-ionized water and then transferred into polyethylene bottles in order to preserve them at +4 °C until analysis time.

Since the concentration of the dissolved Al in rain water samples were below the detection limit of the method ($7.5 \mu\text{M}$), only particulate Al concentrations have been measured as an indicator of dust in the particulate fraction of the precipitation samples. Particulate Al concentrations were determined directly with an Atomic Absorption Spectrophotometer equipped with a deuterium (D2) lamp for background correction (GBC model 906 unit with a FS3000 flame attachment) by using N_2O /acetylene flame. KNO_3 solution at a final concentration of $2000 \text{ mg L}^{-1} \text{ K}^+$ was added to samples and standards to suppress ionization. Almost the same procedure, excluding the suppression of ionization step, has been applied in particulate Fe measurements and air/acetylene flame has been used instead. Monthly field blanks were prepared by pouring 200 mL of double distilled-de-ionized water into the sampling bucket. The mean Fe concentration of 14 field blanks submitted to the same treatment as the precipitation samples was found to be below the detection limit of $1.8 \mu\text{M}$, defined as three times the standard deviation of the blank value. No detectable contamination was found in either the field or laboratory blanks for both Fe_{par} and Al_{par} measurements. The accuracy of the analytical procedure was tested by analyzing standard reference material light sandy soil (CRM 112) of Community Bureau of Reference Brussels (BCR). The overall analytical precision was approximately 4% for Fe and 6% for Al. The samples having very low Fe_{par} concentrations, even lower than the detection limit of the flame AAS method, have been submitted to extra analysis by Graphite Furnace AAS, based on the greater sensitivity and efficiency of this method.

2.7. METEOROLOGICAL PARAMETERS AND AIR MASS BACK TRAJECTORIES

Precipitation was recorded at a sampling rate of half an hour by an Anderrea Meteorological Station installed at the roof of the Institute. Climatically, the Mediterranean region is characterized by generally warm winter temperatures, (November through to February) dominated by rainfall and dry summers (June

through to September). The transitional seasons, spring and autumn are of very variable in length and characteristics. The relatively long spring season (March through May) is noted for periods of unsettled winter-type weather associated with an increased occurrence of North African cyclones; the rest of this period is very similar to that in the summer. Autumn usually lasts only one month (October) and is characterized by an abrupt change from the summer to the unsettled weather of winter (Brody and Nestor, 1980; Özsoy, 1981; Milliman *et al.*, 1992).

Three dimensional, 3-days backward trajectories for air masses arriving at the sampling point on 12 00 UT of the sampling day at levels of 900 and 850 hPa within the boundary layer and 700 and 500 hPa within the free troposphere were calculated for each rainy day. The trajectory model of the European Center for Medium-Range Weather Forecasts (ECMWF) in Reading, England was applied to 3-D analyzed wind fields available from the MARS archive of ECMWF. The method is similar to the method developed by Martin *et al.* (1987) and does not give any information about precipitation events during the excursion of the air masses.

3. Results and Discussion

3.1. PRECIPITATION DATA AND THE MEAN DIRECTIONS OF THE PRECIPITATION CARRYING AIR MASSES

Precipitation data for the sampling period of approximately 17 months were found to be in good agreement with the 30 years (1963–1994) mean climatological rainfall in Mersin (Turkish Meteorological Service, Mersin Station). In the Mersin province, the mean annual precipitation and the number of rainy days were 580 mm and 67.2 respectively, for the period 1963–1994. The annual precipitation corresponding to the period of our sampling (from 5 February 1996 till 5 February 1997) was 540 mm and the number of rainy days was 65 during the same period. Cumulative precipitation belonging for a total of 79 rainy days during the sampling period of February 1996–June 1997 was 710 mm. Minimum and maximum rainfall were 0.2 mm and 87.6 mm, respectively for individual precipitation events (Özsoy, 1999).

In order to identify the mean directions of the air-masses carrying precipitation to the sampling site, the air-mass back trajectories have been classified according to four 90° sectors of arrival. Each trajectory was assigned to the sector in which it spent most of its three days of travel. Figure 1 shows the location of the sampling site, along with the sectors used in trajectory classification of rainy days. Percentage values of mean airflow directions at the 900 hPa barometric pressure level are shown for each sector. The results of the trajectory classification for rainy days performed at 900, 850 hPa levels within the planetary boundary layer (PBL) and at 700, 500 hPa barometric levels within the free troposphere respectively, are also presented in Table II, where the percentage in each direction are given for a total of 79 trajectories during rainy days, of the period February 1996–June 1997 (Özsoy, 1999). The results obtained from this classification are consistent with the ones per-

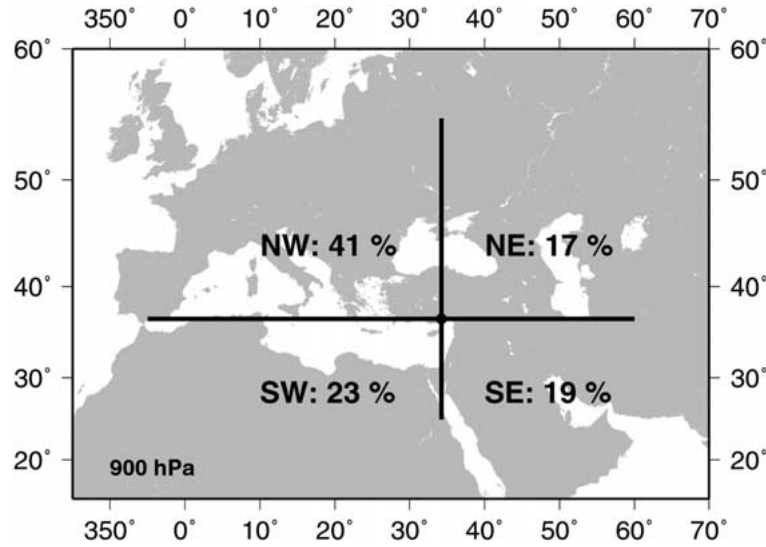


Figure 1. The sectors used in trajectory classification for rainy days with the percentage values of mean airflow directions at the 900 hPa barometric pressure level during February 1996–June 1997 period.

Table II. Comparison of the percentage of mean airflow directions of 79 rainy days at four different (900, 850, 700 and 500 hPa) barometric pressure levels during February 1996–June 1997 with the ones obtained from the classification of 513 consecutive trajectories during August 1991–December 1992, given in parenthesis (after Kubilay, 1996) in Erdemli

hPa	Sector 1 (NE)	Sector 2 (NW)	Sector 3 (SW)	Sector 4 (SE)
900	17 (22)	41 (47)	23 (25)	19 (6)
850	12 (19)	44 (49)	28 (26)	16 (6)
700	1 (9)	47 (57)	49 (32)	3 (2)
500	1 (5)	50 (53)	49 (42)	0 (0)

formed for a total of 513 consecutive trajectories, during August 1991–December 1992 (Kubilay, 1996) for the same location, except that the PBL air-masses from the SE sector had relatively higher frequency and the free troposphere air-masses from the NE sector had relatively lower frequency in the present classification of trajectories for rainy days (Table II).

3.2. STATISTICAL RESULTS AND THE CORRELATIONS BETWEEN THE MEASURED PARAMETERS

Statistics of the measured parameters in Erdemli precipitation are presented in Table III. The measurements of pH, conductivity and particulate Al have been evaluated elsewhere (Özsoy and Saydam, 2000) and the concentration of Fe species, including the former parameters is described here. Due to the highly variable character of atmospheric transport events, the concentration of particulate species; Fe_{par} , Al_{par} and Total Fe in precipitation samples showed large variations, similar to other measured constituents, with standard deviations typically larger than the arithmetic means of these species (Table III). In contrast to the particulate species, the concentration of soluble Fe species; Fe(II) and Fe_{reac} , had smaller variability. However, reducible Fe(III) concentrations were below the detection limit of the applied method in about two thirds of the precipitation samples, due to the uncertainty coming from the subtraction operation. This uncertainty was carried over to the mean concentrations of reducible Fe(III) below the detection limit of the method, yielding high standard deviation values (Table III). Therefore we have used mostly soluble Fe(II) and Fe_{reac} concentrations in our evaluations. The maximum Fe(II) concentrations (0.02–0.42 μM) of Erdemli precipitation is approximately four times higher than the values reported for the precipitation samples collected from the vicinity of Massachusetts Bay and Boston Harbor (0.025–0.10 μM) (Zhuang *et al.*, 1995).

The ratio of soluble Fe(II) to Total Fe has a very wide range of 0.002–64.4% (Geo. mean 1.56%, volume weighted mean 0.31%, Table III). The lowest ratios were obtained for those samples where the mineral dust concentrations were relatively high. The ratio Fe(II)/Total Fe, reported in either aerosol or atmospheric water samples based on laboratory or field studies applying quite different analytical techniques were assembled in Table IV, since the data on iron speciation in the atmosphere is very limited and unfortunately no Fe(II)/Total Fe ratio has been reported for precipitation around the world. The highest ratios have been reported in fog water from a suburb of Zurich, Switzerland, where Fe(II) constituted 20–90% of the Total Fe (Behra and Sigg, 1990), and in fog and cloud-water samples collected in the Los Angeles basin, where Fe(II) constituted 2–55% of the Total Fe (Erel *et al.*, 1993). The ratios reported in these studies are almost on the same order of magnitude. The same type of evaluation is also valid for aerosol samples presented in Table IV, in contrast to our precipitation samples. We have found the widest range of variation in precipitation, varying within four orders of magnitude, and a volume weighted mean ratio which is the lowest among the values reported for other types of atmospheric samples around the world. This result might be attributed to the strong influence of mineral dust transport over the region. Low ratios of Fe(II)/Total Fe belonging to samples with relatively high mineral dust concentrations have lowered the volume weighted mean value of this ratio and caused the scatter in the data. Additionally, the dilution effect, resulting from the

Table III. Statistical results of the measured parameters; pH, conductivity ($\mu\text{S cm}^{-1}$), soluble Fe, particulate Fe, particulate Al concentrations (μM) and the solubility percentage of various iron species in the precipitation samples for the whole sampling period at Erdemli. The number of the samples are given in parenthesis

Parameter	Arit. mean	Geo. mean	VWM	Min.-max.
pH (87)	5.6 ± 0.9	5.5	4.95	3.5–7.6
Conductivity (41)	74.6 ± 79.6	51.4	–	12.9–391.0
Soluble Fe(II) (83)	0.11 ± 0.11	0.06	0.05	BDL–0.42
Reducible Fe(III) (83)	0.03 ± 0.08	0.01	0.01	BDL–0.66
Fe _{reac} (84)	0.14 ± 0.15	0.08	0.07	BDL–1.00
Fe _{filt} (77)	1.47 ± 3.65	0.35	1.03	0.03–26.6
Fe _{par} (84)	22.60 ± 68.60	2.50	16.32	0.07–534.0
Total Fe (80)	24.31 ± 69.83	3.99	17.33	0.12–534.0
Al _{par} (84)	88.77 ± 247.50	15.28	56.31	0.37–1843.0
Fe(II)/Total Fe (%)	6.1 ± 10.8	1.6	0.30	0.002–64.4
Fe _{reac} /Total Fe (%)	7.5 ± 12.6	2.1	0.40	0.005–65.4
Fe _{filt} /Total Fe (%)	25.3 ± 29.2	9.6	6.18	0.018–99.3
Fe _{reac} /Fe _{filt} (%)	3.1 ± 35.4	20.7	6.42	0.11–99.9
Fe(II)/Fe _{reac} (%)	79.8 ± 24.9	71.6	78.20	4.2–100.0
Fe _{par} /Al _{par} (%)	56.6 ± 41.6	4.8	60.00	22.6–161.0

VWM: Volume Weighted Mean.

BDL: Below Detection Limit.

changing volume of precipitation each time, might be responsible for the variation of soluble Fe(II) concentrations and hence for the variation in Fe(II)/Total Fe ratio. It is noteworthy that the volume weighted mean Fe(II)/Total Fe ratio of Erdemli precipitation is even lower than the ratio reported for the Chinese loess particles collected from Luochuan, China (Zhuang *et al.*, 1992) (Table IV). Among the soluble species of iron, Fe(II) was found to be the predominant oxidation state in solution, comprising almost 80% of Fe_{reac}, on the average.

Since the concentration of soluble species is a function of the precipitation volume (Baeyens *et al.*, 1990), the dilution effect on the variability of soluble Fe is displayed by plotting Fe_{reac} concentration against precipitation volume in Figure 2, fitting a hyperbolic relationship $C = A + B/P$, where C: dissolved species concentration, P: precipitation volume, A, B: hyperbolic regression coefficients. The correlation coefficient for the hyperbolic function was significant at the 95% level for Fe_{reac} (0.49), but not for Fe_{filt} (0.083), Fe_{par} (0.097) and Al_{par} (0.086). The main parameter which controls the concentration of the particulate species is identified to be the dust load prior to the rain event, rather than the quantity of precipitation. In particular, the very low correlation (0.083) based on a hyperbolic function of Fe_{filt} seems to indicate that this fraction does not truthfully represent dissolved iron in

Table IV. The Soluble Fe(II)/Total Fe ratio (%) of atmospheric samples reported from various locations around the world. Field based studies (F) are differentiated from laboratory based ones (L) by appropriate notation

Atmospheric sample	Range	VWM	Location	Reference
Fog water (F)	20–90	–	Zurich, Switzerland	Behra and Sigg, 1990
Fog and cloud water (F)	2–55	–	Los Angeles Basin	Erel <i>et al.</i> , 1993
Aerosols (L)	11–100	56	North Pacific	Zhuang <i>et al.</i> , 1992
Aerosols (L)	2.2–49	15 ^a	North Atlantic	Zhu <i>et al.</i> , 1993 ^a
Urban aerosols (L)	–	8.4 ^b	–	Spokes and Jickells, 1996
Urban aerosols (L)	–	6.0 ^c	Mainz, Germany	Dedik <i>et al.</i> , 1992
Urban aerosols (L)	4–11	5.0	Xian, Central China	Zhuang <i>et al.</i> , 1992
Aerosols (L)	–	<1.0	Barbados	Zhu <i>et al.</i> , 1993
Aerosols (L)	0.2–6.5	1.6	Barbados	Zhu <i>et al.</i> , 1997
Aerosols (L)	–	0.9 ^b	North Africa	Spokes and Jickells, 1996
Chinese loess (L)	–	0.4	Luochuan, China	Zhuang <i>et al.</i> , 1992
Rain water (F)	0.002–64.4	0.3	Northeastern Med.	This study

^a This value has been reported as $49 \pm 15\%$ by Zhuang *et al.*, 1992, previously. But the same value was subsequently reported as a typographical error, the correct value being 15% (Zhu *et al.*, 1993).

^b These values belong to the results of photochemical reduction experiments for both North African and urban aerosols.

^c This value has been obtained from the determination of Fe(II) by ion chromatography, the same ratio has been found as 9.4% when Fe(II) was determined by Mössbauer spectrometry.

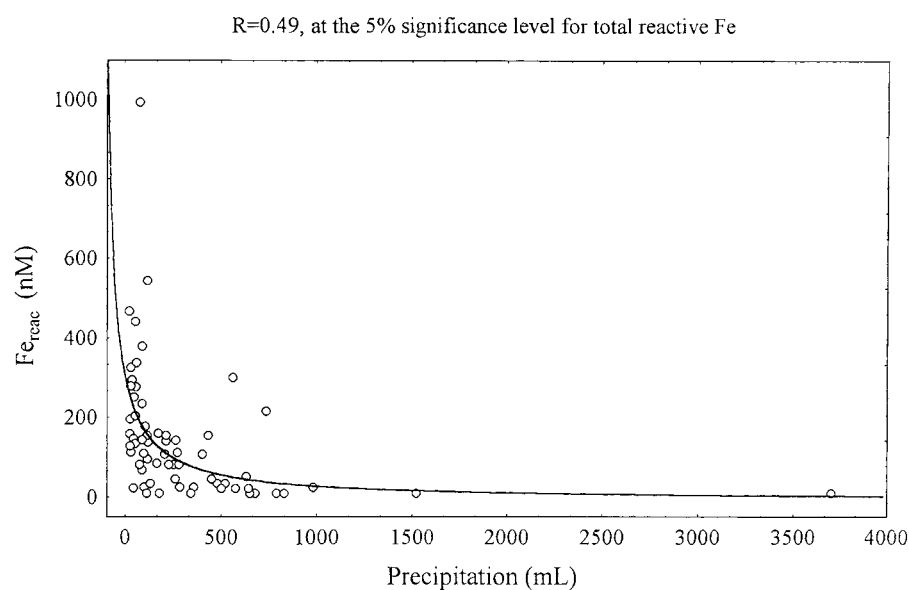


Figure 2. Total reactive Fe (Fe_{reac}) concentration versus precipitation. The best fitted hyperbolic curve is shown by the solid line.

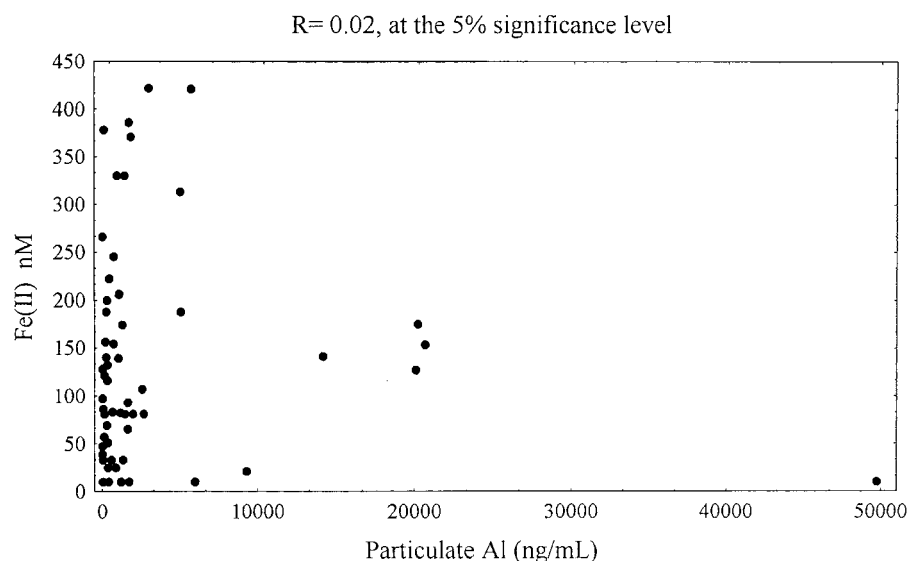


Figure 3. Particulate Al versus soluble Fe(II) concentration in northeastern Mediterranean precipitation.

precipitation, most likely due to the colloidal iron content of Fe_{filt} fraction passing through the $0.45 \mu\text{m}$ pore size filter.

Particulate Al concentration, often used as an indicator of mineral dust load (Prospero and Nees, 1986; Kubilay *et al.*, 2000) is plotted against the Fe(II) concentration in Figure 3 and essentially no correlation ($R = 0.02$) can be found. The same situation is also valid for the relationship between Fe_{reac} and Total Fe ($R = 0.01$) in contrast to the result reported for mineral aerosol samples from Barbados, of which the total soluble iron, Fe_{Ts} concentration is highly correlated to Total Fe ($R^2 = 0.91$, Zhu *et al.*, 1997). As there are very few studies investigating iron solubility in atmospheric samples, we feel obliged to discuss some results of Zhu *et al.* (1997), although the types of atmospheric samples and analytical techniques used in their study are not directly comparable with ours. In their mainly laboratory based study, Zhu *et al.* (1997) have leached aerosol filter samples by a fixed amount of 1 M NaCl solution acidified with HCl for 5 min., and filtered the solution through a $0.2 \mu\text{m}$ filter. They have defined total soluble iron (Fe_{Ts}) as the spectrophotometrically measured concentration in these samples, obtained by adding ferrozine after reduction of the Fe(III) with added hydroxylamine hydrochloride. This definition actually corresponds to our Fe_{reac} fraction of precipitation, except for the pore size of the filter paper used. Moreover, as stated in the discussion concerning Figure 2, the variability in precipitated volume of each sample could be an additional source of variation in the measured analytical concentration of Fe_{reac} , due to the dilution effect in our field based study, as compared to Zhu *et al.* (1997), who have fixed this parameter in the laboratory and simulated atmospheric conditions affecting the dissolution of Fe from a mineral matrix. The two studies

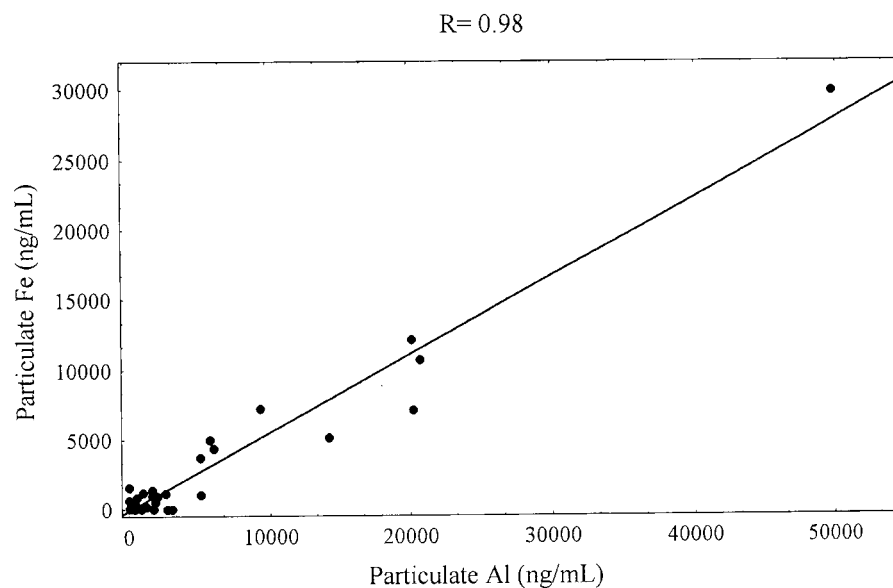


Figure 4. Relationship between the particulate Al and particulate Fe concentrations in precipitation.

are also not comparable with respect to their sampling periods, since the Zhu *et al.* (1997) study was confined to a short time period corresponding to prevailing trade winds at Barbados. The random pattern depicted in Figure 3, clearly demonstrates that the soluble Fe(II) concentration does not generally follow the mineral dust load in the local atmosphere of the eastern Mediterranean.

In contrast to the first relation, a strong correlation ($R = 0.98$) was found between particulate Fe and Al fractions (Figure 4). Atmospheric Al has completely crustal origin, while Fe could have crustal and anthropogenic origins (Church *et al.*, 1990). Assuming that the solubility of Fe and Al is very low due to their dominant crustal origins, the volume weighted mean Fe to Al mass ratio in Erdemli precipitation was calculated depending only on the particulate fractions of the elements. The mean Fe_{par} to Al_{par} mass ratio of 0.60 (Table III) was found to be very close to the ratios reported for global crustal rock (0.68), made of a 1:1 mixture of granite and basalt (Taylor, 1964), and those reported for soil (0.56) (Martin and Whitfield, 1983). This ratio gives us an important indication that the Cilician Basin is under the influence of natural rather than anthropogenic sources.

Random patterns of correlation are also found between reducible Fe(III) and Fe(II) with a correlation coefficient of $R = 0.27$, and Fe_{reac} versus Fe_{filt} with a very low correlation coefficient of $R = 0.10$. Briefly, soluble Fe species (Fe(II), reducible Fe(III), Fe_{reac} , Fe_{filt}) varied independently from each other and no correlation appeared amongst them.

Dependence of soluble Fe(II) on the pH of precipitation is illustrated in Figure 5, suggesting an unpredictable, almost random pattern of soluble Fe(II), with

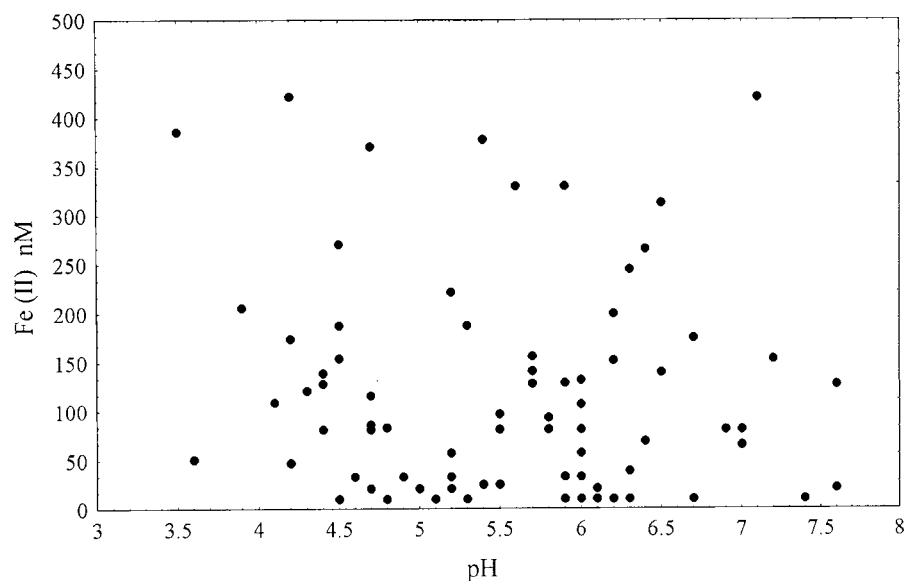


Figure 5. Soluble Fe(II) concentration versus pH of precipitation.

occurrences of high concentrations in the entire pH range of precipitation. A similar pattern is also valid for reducible Fe(III) versus pH. This result clearly demonstrates that soluble Fe(II) and reducible Fe(III) do not depend on the final pH of precipitation, but rather depend on the origin and the mineral content of atmospheric aerosols, in addition to the atmospheric conditions during transport, prior to scavenging by precipitation.

Photochemical processes, which depend on the mineral composition of aerosols impose additional controls on iron speciation and solubility during atmospheric transport (Spokes and Jickells, 1996). In order to investigate the effects of photochemical processes on iron speciation, the data were regrouped according to sampling time of precipitation and the volume weighted mean daytime and nighttime concentrations of the soluble Fe(II), reducible Fe(III) and Fe_{reac} , presented in Table V. The volume weighted mean daytime concentration of Fe(II) is found to be approximately 70% greater than the nighttime values, whereas the mean reducible Fe(III) concentration is almost the same during day and night. Similarly, the mean Fe(II) concentration in daytime samples was reported to be more than twice as high as those in nighttime aerosol samples collected at Barbados (Zhu *et al.*, 1997).

3.3. THE PERCENTAGE OF SOLUBLE IRON SPECIES IN TOTAL IRON POOL OF PRECIPITATION

Precipitation is a very complex solution, and its intensity, deposition flux, pH, ionic strength, particle content, particle size distribution, soluble trace element content, solution volume and the origin of aerosols scavenged from the air, have consid-

Table V. The volume weighted mean of the soluble Fe(II), reducible Fe(III) and Fe_{reac} species in nighttime and daytime precipitation samples in Erdemli (the number of the samples is given in the parenthesis)

Parameter	Nighttime (29)	Daytime (44)
Precipitation (mm)	232.1	233.0
pH	5.1	6.4
Soluble Fe(II) (μM)	0.037	0.064
Reducible Fe(III) (μM)	0.018	0.020
Fe _{reac} (μM)	0.055	0.084
Fe _{filt} (μM)	0.69	1.50

erable variability from one sample to another. These relevant parameters could change even within the same precipitation event, since precipitation chemistry is expected to change dramatically during the course of rainfall (Chester *et al.*, 1997). It is therefore next to impossible to determine all factors controlling the dissolved/particulate speciation of iron in rain water, within given constraints of the analytical procedures and the complexity of precipitation (R. Chester, pers. comm.). Particularly, dissolved-colloidal-particulate speciation of iron in precipitation is somewhat obscure, because of the difficulty in distinguishing these fractions from each other. There seems to be no standard analytical definition of these iron fractions in the literature.

Generally, pH is accepted to be one of the main factors controlling the solubility of aerosol trace elements (Chester *et al.*, 1990, 1993; Lim *et al.*, 1994). Spokes *et al.* (1994) have shown the solubility of iron in atmospheric aerosols to be a function of the aerosol type. Among these diverse factors controlling the solubility of iron, only the pH, the volume of the solution and the particulate iron concentration in precipitation have been measured in our study. In the present section, the solubility of the currently defined iron fractions is investigated with respect to pH and Total Fe (mineral dust load) concentrations, while the reader is referred to Section 3.2 for the effect of solution volume. The solubility of each species, expressed as the percentage of soluble Fe(II), Fe_{reac} and Fe_{filt} (e.g. (soluble Fe(II)/Total Fe) * 100) in precipitation are plotted as a function of pH in Figures 6(a–c), respectively. The dependence of Fe(II)/Total Fe (Figure 6(a)) and Fe_{reac}/Total Fe (Figure 6(b)) with respect to pH of precipitation follow almost the same pattern, since on the average, soluble Fe(II) is by almost 80% comprised of Fe_{reac}. The maximum percentage solubilities of ~65% fall into 4.0–5.5 pH range, and at pH > 5.5 the solubility is always <10% for both of these iron species. In contrast, the percentage solubility of Fe_{filt} (<0.45 μm), classically identified as the dissolved Fe fraction, displayed a much more scattered pattern with values as high as 99%, falling into a relatively wide pH range of 4.0–6.0 in Figure 6(c) and only at pH > 7.0 the solubility is

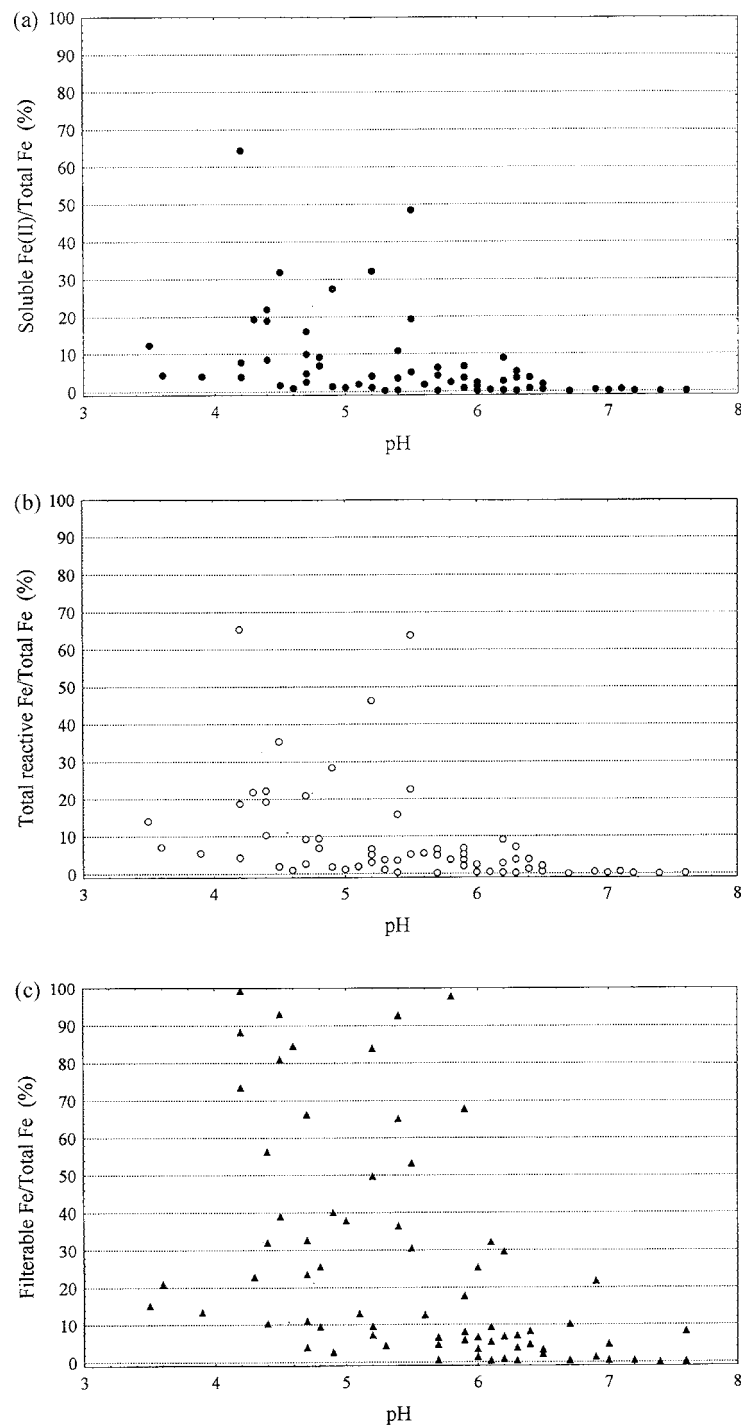


Figure 6. Distribution of the solubility percentage of (a) Fe(II), (b) Fe_{reac}, (c) Fe_{filt} in Erdemli precipitation as a function of pH.

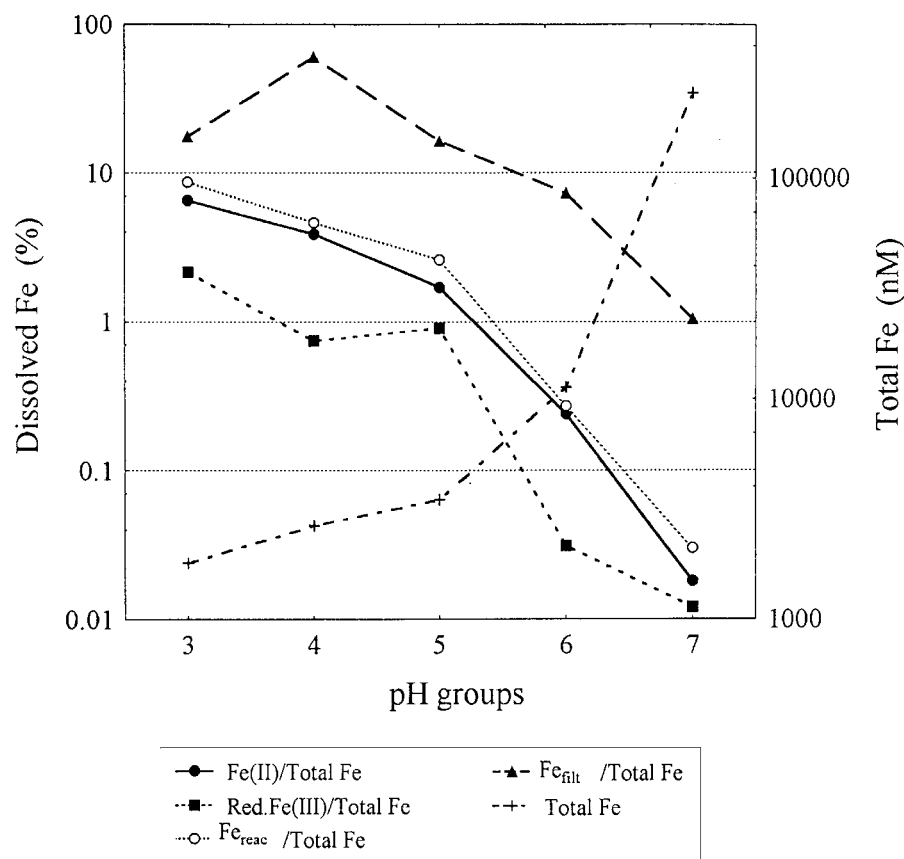


Figure 7. Variation of solubility of various Fe species with respect to pH and total Fe (hence mineral dust) concentration of precipitation.

found to be <10%. In Figure 7, the geometric mean concentration ratios of soluble iron (Fe(II), reducible Fe(III), Fe_{reac} and Fe_{filt}) to Total Fe are plotted against pH groups. The most striking observed feature for all soluble iron fractions is the rapid decrease of solubility above a pH value of 5, in parallel with the rapid increase in mineral dust concentration. In particular, a decrease of more than two orders of magnitude occurs in the solubility of Fe(II) and Fe_{reac} within the pH range of 5–7, whereas this gradient is much smaller (slower) for Fe_{filt} within the same pH range.

The solubility of a trace element is known to be a function of its absolute particle concentration, while its partitioning between solid and dissolved phases depends only on relative magnitude (Honeyman and Santschi, 1988). Being a general indicator of mineral dust load prior to a rain event, the total Fe concentration was considered to be the third parameter controlling the solubility of iron in the present study. In Figures 8(a, b), the solubility percentage of Fe_{reac} and Fe_{filt} respectively are plotted against Total Fe concentration in precipitation. The solubility percentages of these two soluble iron species decrease significantly as the particulate load

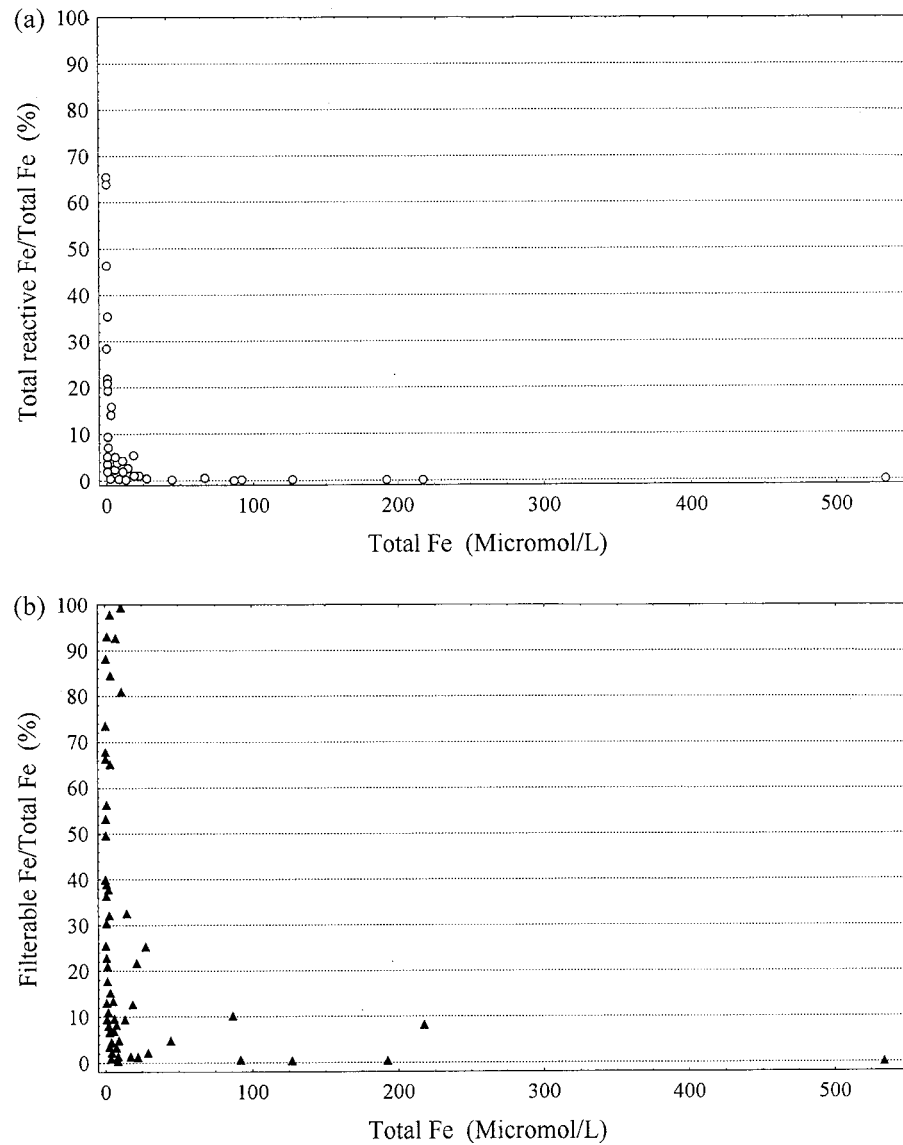


Figure 8. Distribution of (a) $Fe_{\text{reac}}/\text{Total Fe}$, (b) $Fe_{\text{filt}}/\text{Total Fe}$ percentages of precipitation as a function of Total Fe concentration.

increases. Even though the general patterns in Figures 8(a, b) are very similar, the total Fe concentration at which a rapid decrease occurs in the solubility of Fe_{reac} and Fe_{filt} are considerably different from each other. Percentage solubilities of less than 10% occur at Total Fe concentrations of $4 \mu\text{M}$ for Fe_{reac} and $28 \mu\text{M}$ for Fe_{filt} . This big (almost seven fold) difference between the solubility limits of Fe_{reac} and Fe_{filt} justifies the grouping of these solution phase iron fractions as two distinct species. According to Benoit *et al.* (1994) the number of colloids increase with

particulate load, following a 0.7 power law dependence. Therefore when particulate load increases, the number of colloids (including those passing through a 0.45 μm pore size filter) will increase, and the contribution of the solution phase will be overemphasized, as obtained in our Fe_{filt} measurements. Spokes and Jickells (1996) have investigated percentage dissolution of iron from Sahara aerosol in their laboratory based study. They found a significant decrease in percentage dissolution of iron ($<0.2 \mu\text{m}$) with increasing particulate loading, and postulated several possible reasons for this decrease of solution phase Fe, such as preferential readsorption onto particulates and the adsorptive removal by colloids ($>0.2 \mu\text{m}$), the number of which increase with loading. Although our field results are not directly comparable with the laboratory results of Spokes and Jickells (1996), the rapid decrease in the solubility of Fe_{reac} and Fe_{filt} fractions of iron in precipitation with increasing mineral dust load, represents similar behaviour in both studies.

3.4. THE DIFFERENCES BETWEEN 'RED RAIN' AND 'ACIDIC RAIN' EVENTS

Based on the frequency distribution of pH, 28% of the rain samples were found to be acidic (pH < 5.0), about half of which had trajectories showing transport from southeast Europe, the Mediterranean Sea, and from the Balkan Peninsula, while the other half arrived from the Anatolian mainland and other nearby sources. 58% of rain samples were found to be alkaline (pH > 5.6), with trajectories from North Africa and the Middle-East (Özsoy and Saydam, 2000). Because of its CaCO_3 content, mineral dust from these arid regions significantly increased the pH of rain water (Loye-Pilot *et al.*, 1986; Mamane *et al.*, 1987; Losno *et al.*, 1991).

Color identification along with particulate Al measurements of filter samples and air mass back trajectory analysis of the corresponding rainy days revealed 12 outstanding dust transport episodes, associated with 18 'red rain' events, during the entire sampling period. Without exception, the free tropospheric back trajectories for all these events originated from North Africa. The volume weighted mean values of measured parameters associated with acidic versus red rain events are presented in Table VI. Even though the soluble Fe(II), reducible Fe(III) and Fe_{reac} contents of acidic rain are somewhat higher than the corresponding values for red rain, most probably as a result of their lower pH, the difference in the soluble Fe(II), reducible Fe(III) and Fe_{reac} contents of red rain and acidic rain is not statistically significant ($p < 0.05$). In contrast to the soluble Fe(II) and Fe_{reac} species, Fe_{filt} and Fe_{par} contents of red rain are considerably higher than those for acid rain, the difference being two orders of magnitude in the particulate species. The mean Fe_{filt} concentration of red rain is found to be approximately three times higher than acid rain. As noted in Section 2.5, this fraction is usually identified as 'dissolved iron' in the literature but our results have demonstrated that this fraction comprises mostly colloidal iron, while in reality only 6.4% of the Fe_{filt} fraction represents free or soluble iron (Fe_{reac}) based on volume weighted mean (see Table III). Laboratory experiments indicate that colloidal iron that remains suspended in surface waters

Table VI. The volume weighted mean of the measured parameters and the solubility percentage of various iron species in the acidic and red rain events in Erdemli (the number of the samples is given in the parenthesis)

Parameter	Acidic rain (26)	Red rain (18)
Precipitation (mm)	175	72
Color	Grey (10Y 6/1)	Red (10YR 4/3)
Conductivity ($\mu\text{S cm}^{-1}$)	53.5 ± 44.5 (15)	180.4 ± 134.8 (7)
pH	4.4	6.6
Soluble Fe(II) (μM)	0.080	0.066
Reducible Fe(III) (μM)	0.019	0.010
Fe _{reac} (μM)	0.099	0.076
Fe _{filt} (μM)	1.55	4.40
Fe _{par} (μM)	1.19	128.2
Total Fe (μM)	2.74	132.4
Al _{par} (μM)	11.7	433.8
Fe(II)/Total Fe (%)	2.9	0.05
Fe _{reac} /Total Fe (%)	3.6	0.06
Fe _{reac} /Fe _{filt} (%)	6.4	1.74
Fe _{filt} /Total Fe (%)	56.7	3.32
Fe(II)/Fe _{reac} (%)	80.8	86.5

of the ocean could play an important role to supply readily soluble Fe(II) through photoreduction. (Wells and Mayer, 1991; Johnson *et al.*, 1994). Based on our results, we can safely conclude that red rain is quite a rich source of particulate and filterable iron (classically dissolved iron) and it supplies soluble Fe(II) and Fe_{reac} to eastern Mediterranean surface waters, comparable to that supplied by normal (or acidic) rain events.

3.5. CASE STUDIES OF HIGH CONCENTRATION OF SOLUBLE Fe(II) AND TRANSIENT EFFECTS ON SOLUBLE IRON IN PRECIPITATION

High concentrations of soluble Fe(II) were measured in the precipitation samples collected on 7 April 1996 (371 nM) and 17 April 1996 (188 nM). The computed back trajectories arriving at Erdemli on these days suggest different origin of air masses at different levels. The lower level (900 and 850 hPa) trajectories pass over southern Europe and the Mediterranean Sea with potential sources of acidic constituents, while the upper (700 and 500 hPa) levels have North-East African origin (Figure 9). The upper level trajectories reveal upward motions typical of frontal systems (Reiff *et al.*, 1986; Martin *et al.*, 1990), reinforcing the effects of dust transport (Kubilay *et al.*, 2000). Even though particulate Al concentration was

Table VII. The distinction in the measured parameters in subsequently collected precipitation samples upon the instant change in the direction of the corresponding air masses

Sample	A	B
Precipitation (mm)	6.21	8.48
Color of filter	Dull yellow orange (10 YR 7/4)	Gray (10 Y 5/1)
pH	7.6	4.5
Conductivity ($\mu\text{S cm}^{-1}$)	311.0	66.3
Soluble Fe(II) (nM)	21	271
Reducible Fe(III) (nM)	61	30
Fe _{reac} (nM)	82	301
Fe _{filt} (nM)	177	332
Fe _{par} (μM)	128.9	0.52
Total Fe (μM)	129.1	0.85
Al _{par} (μM)	343.6	1.78

high in these samples (69.1 μM and 525.7 μM respectively), the pH values were in the acidic range (4.7 and 5.3 respectively), as a result of mixing between pollutants in the lower troposphere with mineral dust in the upper levels, yielding an expected increase in the soluble Fe(II) concentration.

Greatly differing concentrations of iron were measured in consecutive precipitation samples collected on 21 and 22 March 1997. Unsettled weather conditions prevailed in the region on the first day. Rain started at around 9 pm on the same day and continued until 7 am the next morning. The analysis of sample (A) collected during this event was performed as soon as the rain ceased. After a short break the rain started again and this time it lasted intermittently the whole day with variable wet deposition rates. The second sample (B) was collected between 9 am–10 pm on 22 March 1997 and analysed at night, following the cessation of rain. The results obtained from the analyses of precipitation samples of A and B are presented in Table VII. Air mass trajectories have been calculated according to arrival times of 12210397, 21210397 and 09220397 (the numbers represent UT hours, day, month and year in order) concurrent with the sampling of precipitation, presented in Figures 10(a–c). The computed air mass trajectories arriving at Erdemli on 21 March at 12UT (Figure 10(a)) suggest diverse origins of the air masses according to the final barometric level. The lower level air masses have moved over the Anatolian mainland (900 hPa) and European countries (850 hPa) while the upper (700 and 500 hPa) levels had North-East African origin. The vertical components of the upper level trajectories reveal a notable upward motion, showing the transport of mineral dust by a cyclonic system. Unsettled weather conditions accompanying this cyclonic system resulted in rain commencing at 21 UT on the night of

12170496

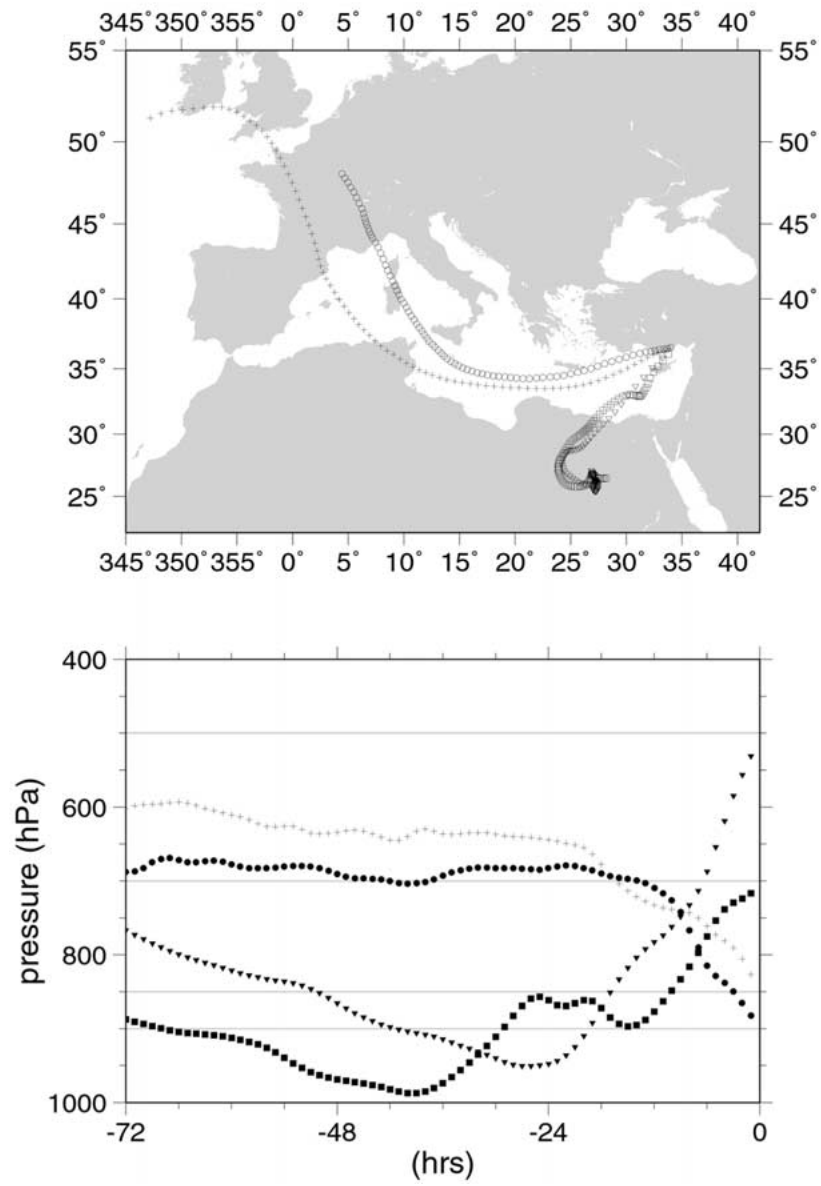


Figure 9. Back trajectories arriving at Erdemli on 17 April 1996.

12210397

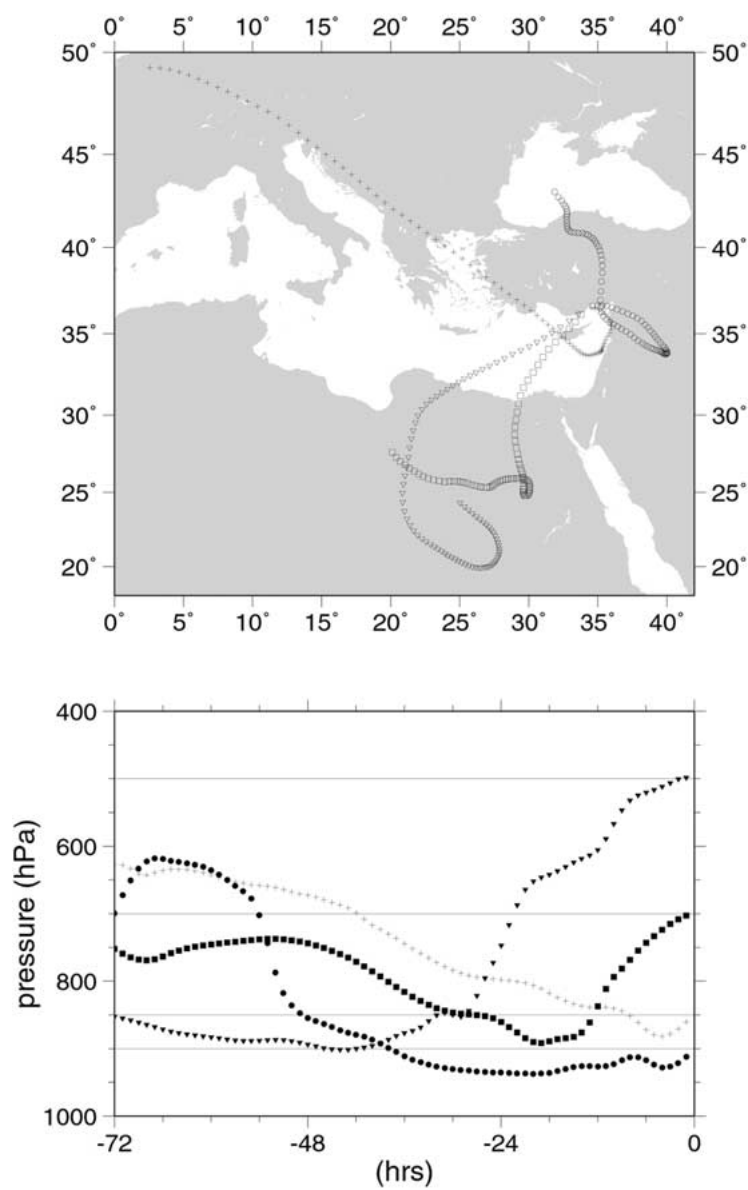
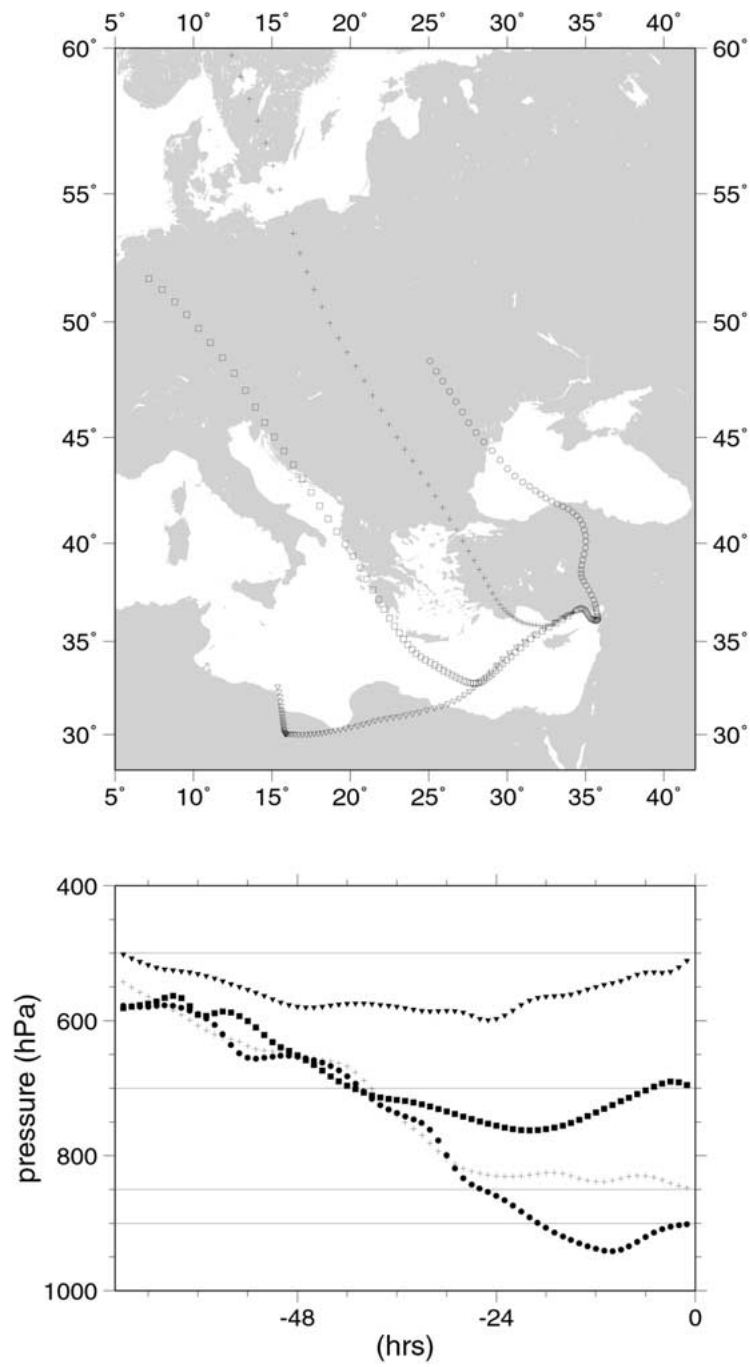


Figure 10a.

21210397

*Figure 10b.*

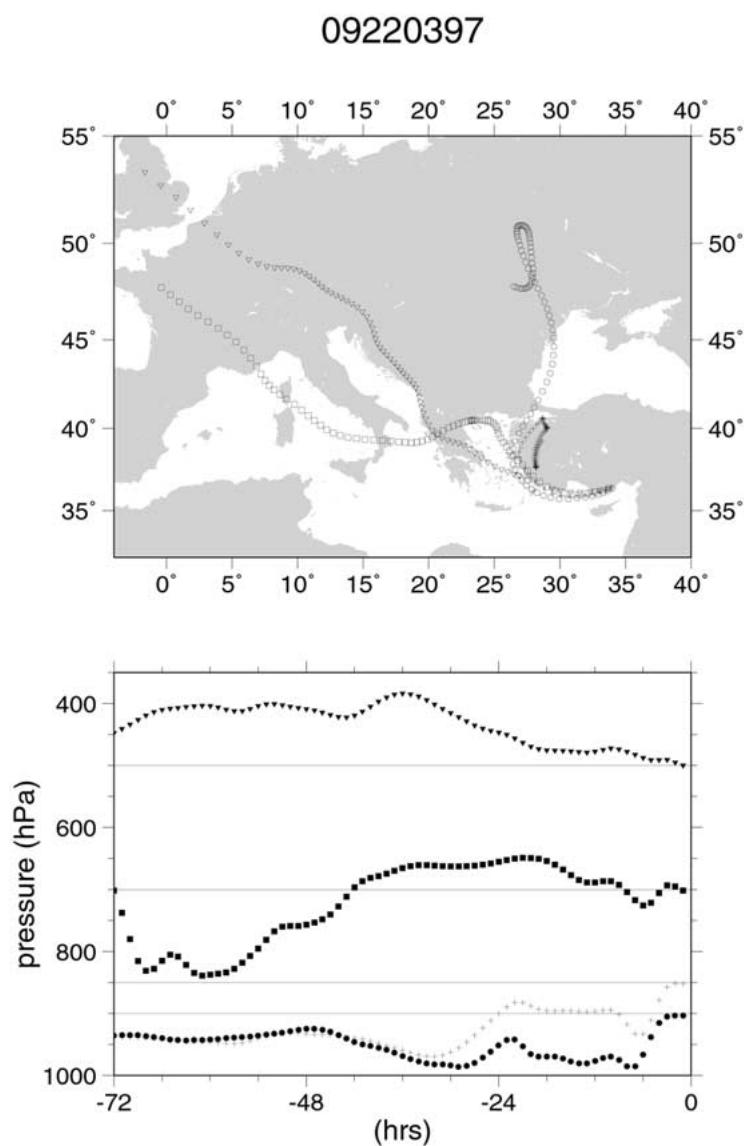


Figure 10c.

Figure 10. Air mass back trajectories calculated according to different arriving times of (a) 12210397, (b) 21210397, (c) 09220397, concurrent to the sampling duration of the consecutively collected precipitation samples.

21 March and resulted in washout of dust from the local atmosphere. The computed air mass trajectories arriving at Erdemli on 21 March at 21UT (Figure 10(b)), at the time of commencement of the first rain (sample A) shows that the air masses at four different pressure levels had already changed their directions, becoming mainly of European origin. The vertical components of the air mass trajectories all reveal descending motion corresponding to anticyclonic motion likely to create stagnant conditions and most probably to allow a build-up of mineral dust in the local atmosphere. As a result, the collected rainwater (sample A) exhibited typical characteristics of Saharan dust with abnormally high values of pH (7.6), particulate aluminium (343.6 μM), particulate iron (128.9 μM) and electrical conductivity (311 $\mu\text{S cm}^{-1}$). The appearance of the particulate matter collected on 0.45 μm diameter membrane filter was very unusual with a distinctly yellowish red color (10 YR 7/4). In contrast to this observation, the air masses corresponding to the precipitation sample B have moved almost isobarically over the potential source regions of acid precipitation (Figure 10(c)), consequently having a low pH (4.5), very low particulate aluminium (1.78 μM), particulate iron (0.52 μM) and relatively low conductivity (66.3 $\mu\text{S cm}^{-1}$), representing more than two orders of magnitude decrease in particulate species compared with the previous sample (Table VII). The color of the particulate matter collected on the filter paper was gray (10 Y 5/1). The soluble species of iron except reducible Fe(III) exhibited the opposite tendency, with sample B having a soluble Fe(II) concentration of an order of magnitude higher than that for sample A, most probably parallel to a decrease in pH. We can not also disregard the effect of photoreductive processes on sample B, since this sample was collected during daytime, while sample A was collected at night-time. This case, showing distinct characteristics for two subsequent precipitation events demonstrates the transient effects of synoptic meteorology, leading to rapid changes in transport direction and associated changes in the geographic origin of air masses, that could result in widely different properties (e.g., pH, conductivity, mineral dust and soluble iron content) of precipitated water.

3.6. WET DEPOSITION FLUX OF TOTAL REACTIVE IRON IN THE NORTHEASTERN MEDITERRANEAN

The precipitation data, originally obtained for each event have been converted into daily quantities so that the wet deposition fluxes can be calculated. The time series of the wet deposition fluxes presented in Figure 11 indicate that the Fe_{reac} and mineral dust fluxes do not vary in a coherent manner. One of the most outstanding cases of increased Fe_{reac} flux occurred on 6 April 1997 when a violent hail storm at the sampling site deposited large ice particles, which stayed on the ground without melting as a result of the cooling that accompanied the event. The total deposition of hail amounted to 25.4 mm of water. The soluble Fe(II) and Fe_{reac} concentrations in the melted hail sample respectively were 188 nM and 216 nM. Despite the possible discrepancies between the measured and actual Fe(II) concen-

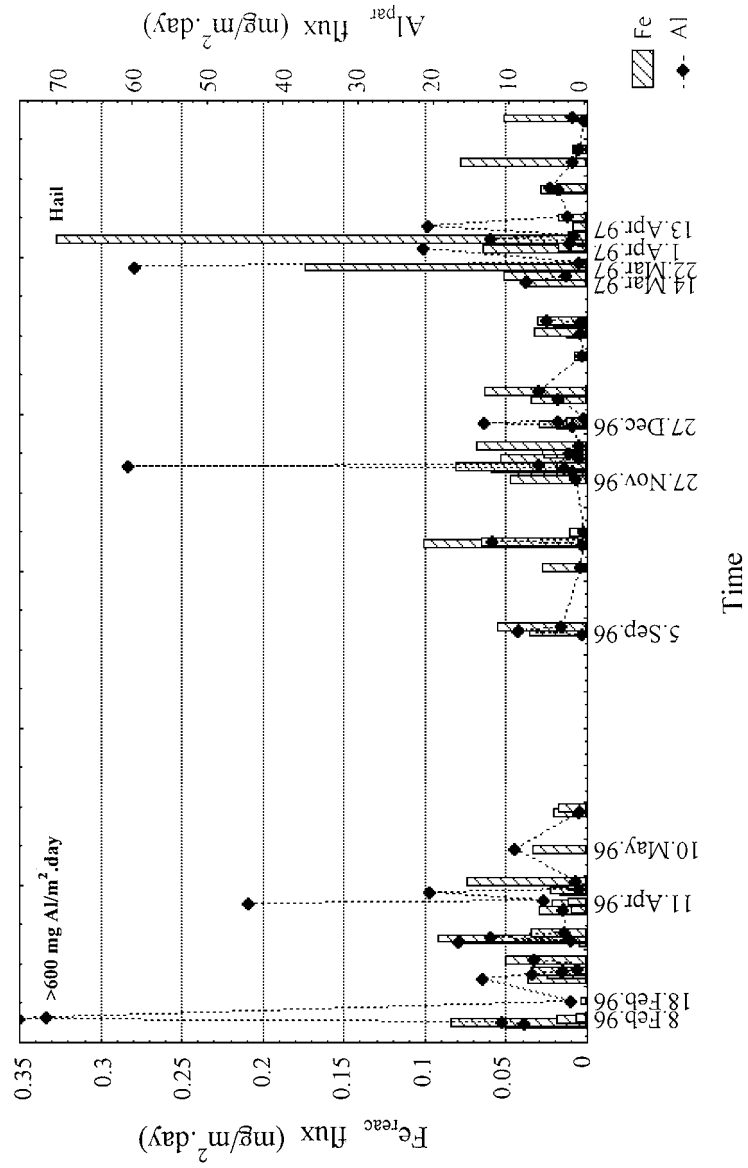


Figure 11. Time series of wet deposition flux of total reactive iron ($F_{Fe^{react}}$) and of particulate Al (Al_{part}) in the Cilician Basin, northeastern Mediterranean.

trations resulting from potential changes in the redox state of Fe during melting, the high Fe_{reac} concentration of the melted precipitation emphasizes the fact that the Fe_{reac} flux ($0.306 \text{ mg/m}^2 \cdot \text{day}$) supplied by a single hail storm to the northeastern Mediterranean coastal waters is twice greater than the maximum Fe_{reac} flux ($0.146 \text{ mg/m}^2 \cdot \text{day}$) supplied by rain. In-cloud processes, such as the strong vertical convection affecting hail formation, particularly taking place within active Cumulonimbus clouds during a storm (Wachter, 1973) and the low pH conditions (Falconer and Falconer, 1980) to which aerosols are exposed during several condensation/evaporation cycles prior to removal by rainout could have increased the solubility of atmospheric iron minerals, leading to high concentrations of Fe(II) and Fe_{reac} in the hail sample.

In order to test whether the total flux of reactive iron is able to support the typical primary production rates in the Levantine Basin, a coarse estimate of the biological requirements for iron is made, using the C:Fe molar ratio of plankton, based on published values for oceanic marine environments, e.g., 10^4 – 10^5 for oceanic plankton (Martin, 1990); 3.3×10^4 (Martin *et al.*, 1989); 5×10^4 for *E. huxleyi* lab culture (Boyd *et al.*, 1996); 3.3×10^5 for primary production in the iron limited equatorial Pacific (Morel *et al.*, 1991). In general, estimates of the minimum and maximum C:Fe (mol:mol) ratio in phytoplankton were estimated to fall between 1.06×10^4 (Morel and Hudson, 1985) and 1.43×10^5 (Anderson and Morel, 1982) (These values were calculated from originally reported Fe:C ($\mu\text{mol:mol}$) ratio of 94 and 7, respectively). Unfortunately, no measurements of the C:Fe ratio are reported so far for the oligotrophic eastern Mediterranean region. Therefore the minimum and maximum C:Fe molar ratio of 1.06×10^4 – 1.43×10^5 were used in the calculation. Based on the maximum rate of primary production in the Levantine Basin reported as $457 \text{ mg C/m}^2 \cdot \text{day}$ (Ediger, 1995), the required flux of Fe is estimated to be 0.015 – $0.20 \text{ mg/m}^2 \cdot \text{day}$. The range of measurements in Figure 11 indicates sufficient quantities of iron, in the relatively scarce bioavailable Fe_{reac} , is supplied to the surface waters of the northeastern Mediterranean by wet deposition, independently of the existence of mineral dust. We should emphasize that the Fe_{reac} deposited at the sea surface is assumed to be biologically available soluble iron fraction for marine organisms. The aqueous chemistry of Fe and its transformations in seawater between redox states is beyond the scope of this work.

4. Conclusions

The analyses of iron species in precipitation samples collected at Erdemli during February 1996–June 1997 clearly demonstrate that precipitation is an important source of soluble Fe(II) to surface waters in the coastal region where this investigation was carried out. Precipitation, particularly in the form of red rain, occurs during spring and fall, supplying large quantities of particular and filterable iron, as well as soluble Fe(II) and Fe_{reac} to the sea surface. No significant difference has been found between normal and red rain samples in terms of soluble iron

[Fe(II) and Fe_{react}] contents. The volume weighted mean Fe_{filt} concentration of the precipitation samples collected during the episodic red rain events was found to be considerably higher.

A strong correlation exists between particulate Fe and Al fractions of precipitation, both of crustal origin. No correlation was found between the soluble and insoluble fractions of iron, or between the soluble species of Fe(II) and reducible Fe(III) and of Fe_{react} and Fe_{filt} concentrations. It was found that the Fe_{filt} fraction, measured by AAS after filtering through $0.45 \mu\text{m}$, and frequently interpreted to be the soluble iron fraction in the literature, represents mostly colloidal iron.

The soluble Fe(II) concentration of precipitation varied independently of the concentration of particulate Fe, hence of the mineral dust load scavenged from the local atmosphere. The geometric mean ratio of soluble Fe(II) and Fe_{react} to Total Fe were found to be 1.6% and 2.1% respectively, while the mean ratio of Fe_{filt} to Total Fe was 9.6%. The volume weighted mean ratios are found to be even lower than the geometric means given above, 0.3%, 0.4% and 6.2%, respectively, in the same order as above. It is noteworthy that the lowest ratios for both species were obtained in precipitation samples with relatively high mineral dust concentration. The percentage of soluble Fe(II) in the total iron pool of precipitation was found to be the lowest among the values reported for other type of atmospheric samples around the world.

High Fe(II) concentrations have been measured both in acid and alkaline rain. The Fe(II) concentration varied independently pH of the precipitation. On the other hand, a positive correlation was found between pH and the particulate fractions of Fe and Al. The elevated pH in precipitation samples in the presence of high atmospheric dust loads can be attributed to the wet scavenging of mineral dust, characterized with high calcite content.

In order to check sufficiency of the atmospheric soluble or bioavailable iron (so called as Fe_{react}) flux to support maximum primary production in the Levantine Basin, an estimate of the flux range was made with values obtained from precipitation in Erdemli were uniformly extended over the Basin. For typical hydrological conditions, the wet deposition flux of Fe_{react} is expected to be sufficient for supporting maximum rates of primary production in the northeastern Mediterranean.

Although the above results reflect the most detailed measurements made to date, they do not pretend to establish a relationship between phytoplankton blooms and mineral dust deposition on the sea surface. Our results support, but do not prove, the hypothesis that increased deposition of iron causes an increase in marine productivity, particularly in a region such as the eastern Mediterranean, despite the lack of iron limitation. Nevertheless, red rain events, following episodic dust transport to the region were found to be an important source of dissolved iron, as well as total reactive iron, for primary producers. In principle, they could support phytoplankton blooms by supplying reactive or bioavailable iron to the sea surface.

Acknowledgements

A substantial part of this study was funded by the Turkish Scientific and Technical Research Council (TÜBİTAK) through the project YDABÇAG-462/G. We thank Emin Özsoy of the IMS-METU, for his help in reviewing the manuscript, as well as for making the ECMWF trajectory analyses, through collaboration with the Turkish State Meteorological Office.

References

- Anderson, M. A. and Morel, F. M. M., 1982: The influence of aqueous iron chemistry on the uptake of iron by coastal diatom *Thalassiosira weissflogii*, *Limnol. Oceanogr.* **27**, 789–813.
- Baeyens, W., Dehairs, F., and Dedeurwaerder, H., 1990: Wet and dry deposition fluxes above the North Sea, *Atmos. Environ.* **24A** (7), 1693–1703.
- Behra, P. and Sigg, L., 1990: Evidence for redox cycling of iron in atmospheric water droplets, *Nature* **344**, 419–421.
- Benoit, G., Oktay-Marshall, S. D., Cantu, A., Hood, E. M., Coleman, C. H., Çorapçıoğlu, M. O., and Santschi, P. H., 1994: Partitioning of Cu, Pb, Ag, Zn, Fe, Al and Mn between filter-retained particles, colloids and solution in six Texas estuaries, *Mar. Chem.* **45**, 307–336.
- Bergametti, G., Remoudaki, E., Losno, R., Steiner, E., Chatenet, B., and Buat-Menard, P., 1992: Source, transport and deposition of atmospheric phosphorus over the northwestern Mediterranean, *J. Atmos. Chem.* **14**, 501–513.
- Box, J. D., 1984: Observations on the use of iron(II) complexing agents to fractionate the total filterable iron in natural water samples, *Water Res.*, **18** (4), 397–402.
- Boyd, P. W., Muggli, D. L., Varela, D. E., Goldblatt, R. H., Chretien, R., Orians, K. J., and Harrison, P. J., 1996: *In vitro* iron enrichment experiments in the NE subarctic Pacific, *Marine Ecology Progress Series* **136**, 179–193.
- Brody, L. R. and Nestor, M. J. R., 1980: Handbook for Forecasters in the Mediterranean, Part 2. Regional forecasting aids for the Mediterranean Basin, Technical Report TR 80-10, pp. VII–1; VII–13, Naval Environmental Prediction Research Facility, Monterey, California.
- Bruland, K. W., Donat, J. R., and Hutchins, D. A., 1991: Interactive influences of bioactive trace metals on biological production in oceanic waters, *Limnol. Oceanogr.* **36** (8), 1555–1577.
- Chester, R., Lin, F. J., and Murphy, K. J. T., 1989: A three stage sequential leaching scheme for the characterisation of the sources and environmental mobility of trace metals in the marine aerosol, *Environ. Tech. Letts.* **10**, 887–900.
- Chester, R., Nimmo, M., Murphy, K. J. T., and Nicholas, E., 1990: Atmospheric trace metals transported to the Western Mediterranean: Data from a station on Cap Ferrat, EROS 2000 2nd workshop, *Water Pollution Research Report* 20, pp. 597–612, March 90, Blanes, Spain.
- Chester, R., Murphy, K. J. T., Lin, F. J., Berry, A. S., Bradshaw, G. A., and Corcoran, P. A., 1993: Factors controlling the solubilities of trace metals from non-remote aerosols deposited to the sea surface by the 'dry' deposition mode, *Mar. Chem.* **42**, 107–126.
- Chester, R., Nimmo, M., and Corcoran, P. A., 1997: Rain water-aerosol trace metal relationships at Cap Ferrat: A coastal site in the Western Mediterranean, *Mar. Chem.* **58**, 293–312.
- Church, T. M., Arimoto, R., Barrie, L. A., Dehairs, F., Dulac, F., Jickells, T. D., Mart, L., Sturges, W. T., and Zoller, W. H., 1990: The long-range atmospheric transport of trace elements: A critical evaluation, in A. H. Knap (ed.), *The Long-Range Atmospheric Transport of Natural and Contaminant Substances*, Kluwer Academic Publishers, The Netherlands, pp. 37–58.
- Dedik, A. N., Hoffmann, P., and Enslin, J., 1992: Chemical characterization of iron in atmospheric aerosols, *Atmos. Environ.* **26**, 2545–2548.

- De Haan, H., Veldhuis, M. J. W., and Moed, J. R., 1985: Availability of dissolved iron from Tjeukemeer, The Netherlands, for iron-limited growing *Scenedesmus quadricauda*, *Water Res.* **19**, 235–239.
- De Haan, H. and De Boer, T., 1986: Geochemical aspects of aqueous iron, phosphorus and dissolved organic carbon in the humic Lake Tjeukemeer, The Netherlands, *Freshwater Biology* **16**, 661–672.
- Donaghay, P. L., Liss, P. S., Duce, R. A., Kester, D. R., Hanson, A. K., Villareal, T., Tindale, N. W., and Gifford, D. J., 1991: The role of episodic atmospheric nutrient inputs in the chemical and biological dynamics of oceanic ecosystems, *Oceanography* **4** (2), 62–70.
- Duce, R. A. and Tindale, N. W., 1991: Atmospheric transport of iron and its deposition in the ocean, *Limnol. Oceanogr.* **36** (8), 1715–1726.
- Erel, Y., 1991: Transport of natural lead and cadmium in rivers: Global flux implications, PhD Thesis, California Inst. Technol.
- Erel, Y., Pehkonen, S. O., and Hoffmann, M. R., 1993: Redox chemistry of iron in fog and stratus clouds, *J. Geophys. Res.* **98** (10), 18 423–18 434.
- Falconer, R. E. and Falconer, P. D., 1980: Determination of cloud water acidity at a mountain observatory in the Adirondack Mountains of New York State, *J. Geophys. Res.* **85**, 7465–7470.
- Faust, B. C., 1994: Photochemistry of clouds, fogs and aerosols, *Env. Sci. Tech.* **28**, 217–222.
- Finden, D. A. S., Tipping, E., Jaworski, G. H. M., and Reynolds, C. S., 1984: Light-induced reduction of natural iron (III) oxide and its relevance to phytoplankton, *Nature* **309**, 783–784.
- Guieu, C., Martin, J. M., Thomas, A. J., and Poulichet, F. E., 1991: Atmospheric versus river inputs of metals to the Gulf of Lions. Total concentrations, partitioning and fluxes, *Mar. Poll. Bull.* **22** (4), 176–183.
- Guieu, C., Zhang, J., Thomas, A. J., Martin, J. M., and Brun-Cotton, J. C., 1993: Significance of the atmospheric fallout upon the upper layer water chemistry of the northwestern Mediterranean, *J. Atmos. Chem.* **17**, 45–60.
- Guerzoni, S., Chester, R., Dulac, F., Herut, B., Loye-Pilot, M. D., Measures, C., Migon, C., Molinaroli, E., Moulin, C., Rossini, P., Saydam, C., Soudine, A., and Ziveri, P., 1999: The role of atmospheric deposition in the biogeochemistry of the Mediterranean Sea, *Progress in Oceanography* **44**, 147–190.
- Heaney, S. I. and Davison, W., 1977: The determination of ferrous iron in natural waters with 2,2'-bipyridyl, *Limnol. Oceanogr.* **22**, 753–760.
- Honeyman, B. D. and Santschi, P. H., 1988: Metals in aquatic systems, *Environ. Sci. Technol.* **22**, 862–871.
- Johnson, K. S., Coale, K. H., Elrod, V. A., and Tindale, N. W., 1994: Iron photochemistry in seawater from the equatorial Pacific, *Mar. Chem.* **46**, 319–334.
- Kester, D. R., 1994: Marine redox cycle of iron, in Iron Speciation and its Biological Availability in Seawater: A Workshop, Bermuda Biological Station for Research, 1–5 May, 1994, Participant Abstracts, pp.45–46.
- Kremling, K. and Streu, P., 1993: Saharan dust influenced trace element fluxes in deep north Atlantic subtropical waters, *Deep-Sea Res.* **40**, 1155–1168.
- Kubilay, N., 1996: The Composition of atmospheric aerosol over the eastern Mediterranean: The coupling of geochemical and meteorological parameters, PhD Thesis, IMS-METU, Turkey, p. 214.
- Kubilay, N., Nickovic, S., Moulin, C., and Dulac, F., 2000: An illustration of the transport and deposition of mineral dust onto the eastern Mediterranean, *Atmos. Environ.* **34** (8), 1293–1303.
- Krom, M. D., Kress, N., and Brenner, S., 1991: Phosphorus limitation of primary productivity in the eastern Mediterranean, *Limnol. Oceanogr.* **36**, 424–432.
- Lengweiler, H., Buser, W., and Feitknecht, W., 1961: Determination of the solubility of iron(III) hydroxide with iron-59. II. The state of very small amounts of iron(III) hydroxide in aqueous solution, *Helv. Chim. Acta.* **44**, 805–811.

- Lim, B., Jickells, T. D., Colin, J. L., and Losno, R., 1994: Solubilities of Al, Pb, Cu and Zn in rain sampled in the marine environment over the North Atlantic Ocean and Mediterranean Sea, *Global Biogeochemical Cycles* **8**, 349–362.
- Losno, R., Bergametti, G., Carlier, P., and Mouvier, G., 1991: Major ions in marine rainwater with attention to sources of alkaline and acidic species, *Atmos. Environ.* **25A**, 763–770.
- Loye-Pilot, M. D., Martin, J. M., and Morelli, J., 1986: Influence of Saharan dust on the rain acidity and atmospheric input to the Mediterranean, *Nature* **321**, 427–428.
- Mamane, Y., Dayan, U., and Miller, J. M., 1987: Contribution of alkaline and acidic sources to precipitation in Israel, *Sci. Tot. Environ.*, **61**, 15–22.
- Martin, D., Mithieux, C., and Strauss, B., 1987: On the use of the synoptic vertical wind component in a transport trajectory model, *Atmos. Environ.* **21**, 45–52.
- Martin, D., Bergametti, G., and Strauss, B., 1990: On the use of the synoptic vertical velocity in trajectory model: validation by geochemical tracers, *Atmos. Environ.* **24A**, 2059–2069.
- Martin, J. H. and Fitzwater, S. E., 1988: Iron deficiency limits phytoplankton growth in the northeast Pacific subarctic, *Nature* **331**, 341–343.
- Martin, J. H., Fitzwater, S. E., Gordon, R. M., and Broenkow, W. W., 1989: VERTEX: phytoplankton/iron studies in the Gulf of Alaska, *Deep-Sea Res.* **36**, 649–680.
- Martin, J. H., Fitzwater, S. E., and Gordon, R. M., 1990: Iron deficiency limits phytoplankton growth in Antarctic waters. *Global Biogeochemical Cycles* **4**, 5–12.
- Martin, J. H., Gordon, R. M., and Fitzwater, S. E., 1991: The case for iron, *Limnol. Oceanogr.* **36** (8), 1793–1803.
- Martin, J. M. and Whitfield, M., 1983: The significance of the river input of chemical elements to the ocean, in C. S. Wong, E. Boyle, K. W. Bruland, J. D. Burton, and E. D. Goldberg (eds), *Trace Metals in Seawater*, Plenum Publishing, New York. Corporation, pp. 265–296.
- Migon, C. and Sandroni, V., 1999: Phosphorus in rainwater: Partitioning inputs and impact on the surface coastal ocean, *Limnol. Oceanogr.* **44** (4), 1160–1165.
- Mill, A. J. B., 1980: Colloidal and macromolecular forms of iron in natural waters 1: A review, *Env. Tech. Lett.* **1**, 97–108.
- Milliman, J. D., Jeftic, L., and Sestini, G., 1992: The Mediterranean Sea and climate change – An overview, in L. Jeftic, J. D. Milliman, and G. Sestini (eds), *Climatic Change and Mediterranean*, UNEP, pp. 1–14.
- Morel, F. M. M. and Hudson, R. J. M., 1985: The geobiological cycle of trace elements in aquatic systems: Redfield revisited, in W. Stumm (ed.), *Chemical Processes in Lakes*, Wiley-Interscience, New York, pp. 251–281.
- Morel, F. M. M., Hudson, R. J. M., and Price, N. M., 1991: Limitation of productivity by trace metals in the sea, *Limnol. Oceanogr.* **36**, 1742–1755.
- O’Sullivan, D. W., Hanson, A. K., Miller, W. L., and Kester, D. R., 1991: Measurement of Fe(II) in surface water of the equatorial Pacific, *Limnol. Oceanogr.* **36**, 1727–1741.
- Özsoy, E., 1981: On the Atmospheric Factors Affecting the Levantine Sea. European Centre for Medium Range Weather Forecasts, Technical Report No. 25, p. 29.
- Özsoy, T., 1999: Kilikya Baseni kıyısı sistemine taşınan atmosferik kirleticilerin kaynaklarının belirlenmesi, Atmosferik girdilerin deniz ekosistemi üzerine olan etkileri, Doktora Tezi, Mersin Üniversitesi, Fen Bilimleri Enstitüsü, Mersin, 209 sayfa.
- Özsoy, T. and Saydam, A. C., 2000: Acidic and alkaline precipitation in the Cilician Basin, northeastern Mediterranean Sea, *Sci. Tot. Environ.*, **253** (1–3), 95–111.
- Powell, R. T. and Landing, W. M., 1994: Colloidal iron: Oceanic and estuarine size distributions and reactivity, in Iron Speciation and its Biological Availability in Seawater: A Workshop, Bermuda Biological Station for Research, 1–5 May, 1994, Participant Abstracts, pp. 67–68.
- Prospero, J. M., 1981: Eolian transport to the world oceans, in C. Emiliani (ed.), *The Sea* **7**, Wiley, New York, pp. 801–874.

- Prospero, J. M. and Nees, R. T., 1986: Deposition rate of particulate and dissolved Aluminum derived from Saharan dust in precipitation at Miami, Florida, *J. Geophys. Res.* **92**, 14723–14731.
- Quetel, C. R., Remoudaki, E., Davies, J. E., Miquel, J. C., Fowler, S. W., Lambert, C. E., Bergametti, G., and Buat-Menard, P., 1993: Impact of atmospheric deposition on particulate iron flux and distribution in northwestern Mediterranean waters, *Deep Sea Res.* **40**, 989–1002.
- Pandis, S. N. and Seinfeld, J. H., 1989: Mathematical modeling of acid deposition due to radiation fog, *J. Geophys. Res.* **94**, 12 911–12 923.
- Reiff, J., Forbes, G. S., Spicksma, F. Th. M., and Reynders, J. J., 1986: African dust reaching northwestern Europe: A case study to verify trajectory calculations, *Journal of Climate and Applied Meteorology* **25**, 1543–1567.
- Rich, H. W. and Morel F. M. M., 1990: Availability of well-defined iron colloids to the marine diatom *Thalassiosira weissflogii*, *Limnol. Oceanogr.* **35**, 652–662.
- Saydam, A. C., 1996: Can we predict harmful algae bloom, UNESCO/IOC *Harmful Algae Newsletter* **15**, 5–9.
- Sheldon, R. W., 1972: Size separation of marine seston by membrane and glass-fibre filters, *Limnol. Oceanogr.* **17**, 494–498.
- Sivan, O., Erel, Y., Mandler, D., and Nishri, A., 1998: The dynamic redox chemistry of iron in the epilimnion of lake Kinneret (Sea of Galilee), *Geochim. Cosmochim. Acta* **62**, 565–576.
- Snell, F. D., Snell, C. T., and Snell, C. A., 1959: *Colorimetric Methods of Analysis*, Vol. IIA. Van Nostrand, Princeton.
- Spokes, L. J., Jickells, T. D., and Lim, B., 1994: Solubilisation of aerosol trace metals by cloud processing: A laboratory study, *Geochim. Cosmochim. Acta* **58** (15), 3281–3287.
- Spokes, L. J. and Jickells, T. D., 1996: Factors controlling the solubility of aerosol trace metals in the atmosphere and on mixing into seawater, *Aquatic Geochemistry* **1**, 355–374.
- Stumm, W. and Lee, G. F., 1960: The chemistry of aqueous iron, *Schweiz. Z. Hydrol.* **22**, 295–319.
- Sulzberger, B., 1992: The role of heterogeneous photochemical reactions for the formation of dissolved iron species in aquatic systems, in J. M. Martin and H. Barts (eds), *Water Pollution Research Reports 13*, EROS 2000, Fourth Workshop on the North-West Mediterranean Sea, Commission of the European Communities, Brussels, pp. 183–186.
- Sulzberger, B. and Laubscher, H., 1995: Reactivity of various types of iron(III) (hydr)oxides towards light-induced dissolution, *Mar. Chem.* **50**, 103–115.
- Talbot, R. W., Harris, R. C., Brawl, E. V., Gregory, G. L., Debaucher, D. I., and Beck, S. M., 1986. Distribution and geochemistry of aerosols in the tropical North Atlantic troposphere: Relationship to Saharan dust, *J. Geophys. Res.* **91**, 5173–5182.
- Taylor, S. R., 1964: Abundance of chemical elements in the continental crust: A new table, *Geochim. Cosmochim. Acta* **28**, 1273–1285.
- Uematsu, M., 1987: Study of the continental material transported through the atmosphere to the ocean, *Journal of Oceanographic Society, Japan* **43**, 395–401.
- UNEP (United Nations Environment Programme), 1995: Manual for the Geochemical Analyses of Marine Sediments and Suspended Particulate Matter. Reference Methods for Marine Pollution Studies. No.63.
- Wachter, H., 1973: *Meteorology, Forecasting the Weather*, Collins Publisher, New York, p. 128.
- Wells, M. L. and Mayer, L. M., 1991: The photoconversion of colloidal iron oxyhydroxides in seawater, *Deep-Sea Res.* **38**(11), 1379–1395.
- Wells, M. L., Mayer, L. M., and Guillard, R. R. L., 1991: Evaluation of iron as a triggering factor for red tide blooms, *Marine Ecology Progress Series* **69**, 93–102.
- Wells, M. L., Price, N. M., and Bruland, K. W., 1995: Iron chemistry in seawater and its relationship to phytoplankton: A workshop report, *Mar. Chem.* **48**, 157–182.
- Zhu, X. R., Prospero, J. M., Millero, F. J., Savoie, D. L., and Brass, G. W., 1992: The solubility of ferric ion in marine mineral aerosol solutions at ambient relative humidities, *Mar. Chem.* **38**, 91–107.

- Zhu, X. R., Prospero, J. M., Savoie, D. L., Millero, F. J., Zika, R. G., and Saltzman, E. S., 1993: Photoreduction of iron(III) in marine mineral aerosol solutions, *J. Geophys. Res.* **98**(D5), 9039–9046.
- Zhu, X. R., Prospero, J. M., and Millero, F. J., 1997: Diel variability of soluble Fe(II) and soluble total Fe in North African dust in the trade winds at Barbados, *J. Geophys. Res.* **102** (D17), 21 297–21 306.
- Zhuang, G., Duce, R. A., and Kester, D. R., 1990: The dissolution of atmospheric iron in surface seawater of the open ocean, *J. Geophys. Res.* **95**, 16207–16216.
- Zhuang, G., Yi, Z., Duce, R. A., and Brown, P. R., 1992: Link between iron and sulphur cycles suggested by detection of Fe(II) in remote marine aerosols, *Nature* **355**, 537–539.
- Zhuang, G., Yi, Z. and Wallace, G. T., 1995: Iron(II) in rainwater, snow and surface seawater from a coastal environment, *Mar. Chem.* **50**, 41–50.